Higgs studies on full Run2 differential measurements with ATLAS

Lailin Xu
Brookhaven National Laboratory
On behalf of the ATLAS Collaboration

Higgs Hunting 2019, July 29-31, Orsay-Paris

Introduction

- Why fiducial and differential cross section measurements?
  - Important test of the SM (e.g. perturbative QCD calculations)
  - Minimal model dependence, easier for reinterpretation (EFT, couplings, etc)
  - Sensitive probe to physics beyond the SM
    - Low p_T region sensitive to light quark Yukawa couplings
    - High p_T region sensitive to potential new particles in ggF loop

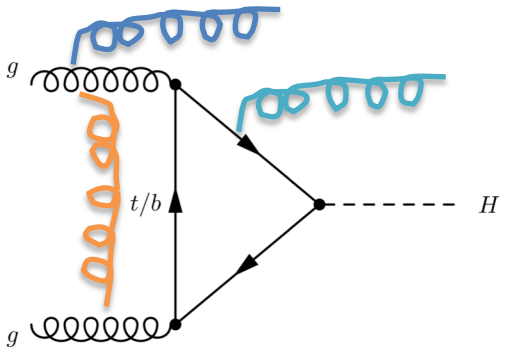

- First full run 2 (139 fb^{-1}) measurements from ATLAS:
  - Fiducial cross sections in H→ZZ*→4l and H→γγ
  - Differential cross sections:
    - p_T^{4l} , N_{jets} in 4l fiducical region
    - $p_T^{\gamma\gamma}$, $|y_{\gamma\gamma}|$, N_{jets}, p_T^{j1}, m_{jj}, $\Delta\phi_{jj}$ in γγ fiducial region
  - Combination of H→ZZ*→4l and H→γγ :
    - Total cross section
    - p_T^H in extrapolated phase space
  - Interpretations of differential measurements

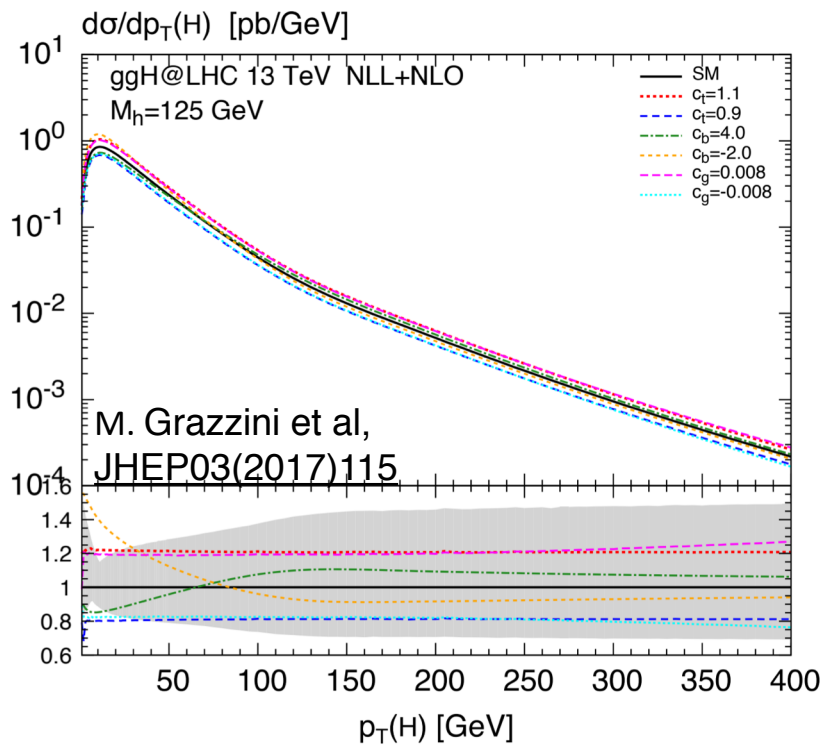

Theoretical predictions

- MC generators and cross-section predictions

Process	Generators	Accuracy	Cross-section normalizations	Fraction [%]
ggF	Powheg-Box v2 (NNLOPS)	NNLO QCD in $\lvert y_H \rvert$	N^3LO in QCD, NLO EW corrections	87.2
	MG5_aMC@NLO FxFx	0,1,2jet @NLO		
VBF	Powheg-Box v2	NLO QCD	(approx.) NNLO in QCD, NLO in EW	6.8
VH	Powheg-Box v2 (MiNLO)	NLO QCD	qq/qg: NNLO in QCD, NLO in EW; gg: NLO+NLL in QCD	4.0
ttH	Powheg-Box v2	NLO QCD	NLO in QCD, NLO in EW	1.1
tH	MG5_aMC@NLO	NLO QCD	NLO in QCD	
bbH	MG5_aMC@NLO	NLO QCD	NNLO (NLO) in QCD for 5FS (4FS)	0.9

NLO QCD MC is the minimum requirement

Cross sections taken from the state-of-the-art theory predictions

How to measure fiducial and differential cross sections

- General method:

$$\sigma_{\text{fid}} = \frac{N^{\text{sig}}}{c_{\text{fid}}\mathcal{L}_{\text{int}}}$$

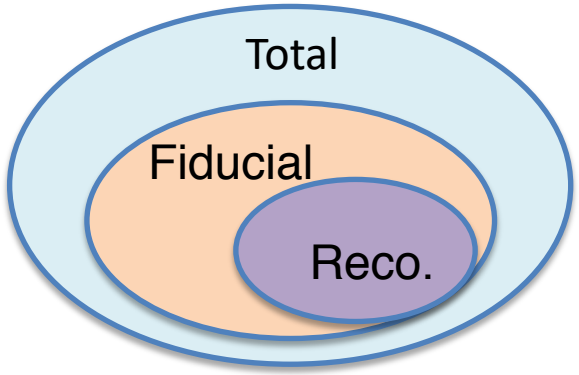

- Signal extraction, N_{sig}:
  - Signal events extracted from a m_{4l} or $m_{\gamma\gamma}$ fit, given the excellent resolution
  - Background constrained from data sideband

- Correction factor (unfolding), c_{fid}:
  - To unfold detector efficiency and resolution effect
  - Obtained from MC simulation: ~49% for 4l, ~71% for $\gamma\gamma$
    - Leakage from outside fid. region is found to be small, ~2%

For fiducial measurements:

$$C_{\text{fid}} = \frac{N_{Reco.}}{N_{Fid.}}$$

- Differential cross section:
  - In each bin of a differential distribution, signal events are extracted from a m_{4l} or $m_{\gamma\gamma}$ fit
  - Unfolding:
    - Response matrix method (default method for 4l)
    - Bin-by-bin correction factor method (default method for $\gamma\gamma$)

$H \rightarrow ZZ^* \rightarrow 4l$

ATLAS-CONF-2019-025

Reconstructed observables

- 316 events observed in $115 < m_{4l} < 130$ GeV
  - With expected signal events: 206 $\pm$13
  - ZZ background constrained from data sideband in a simultaneous fit → reduce modelling uncertainties
    - Expected total background: 97 $\pm$ 6

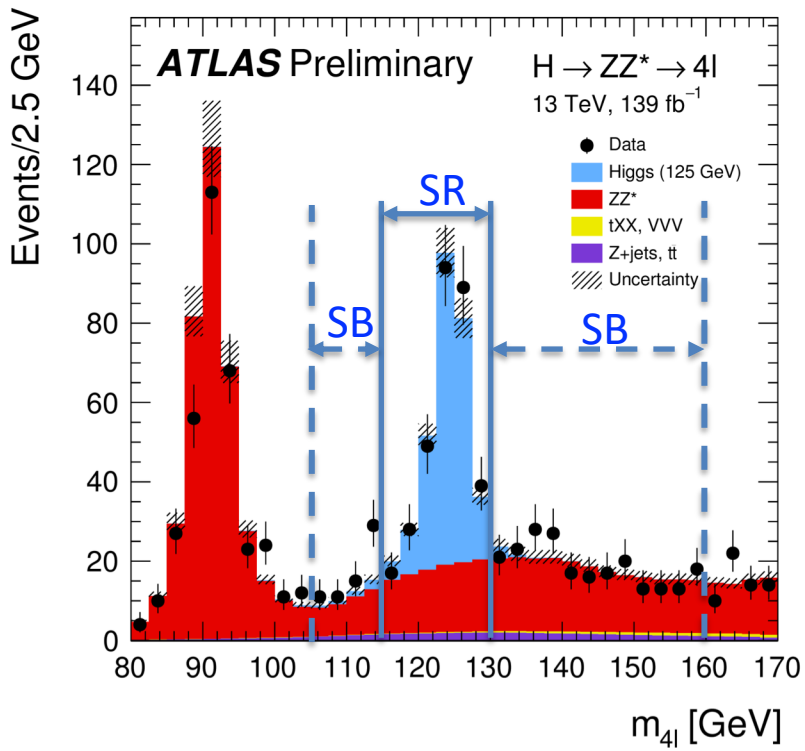

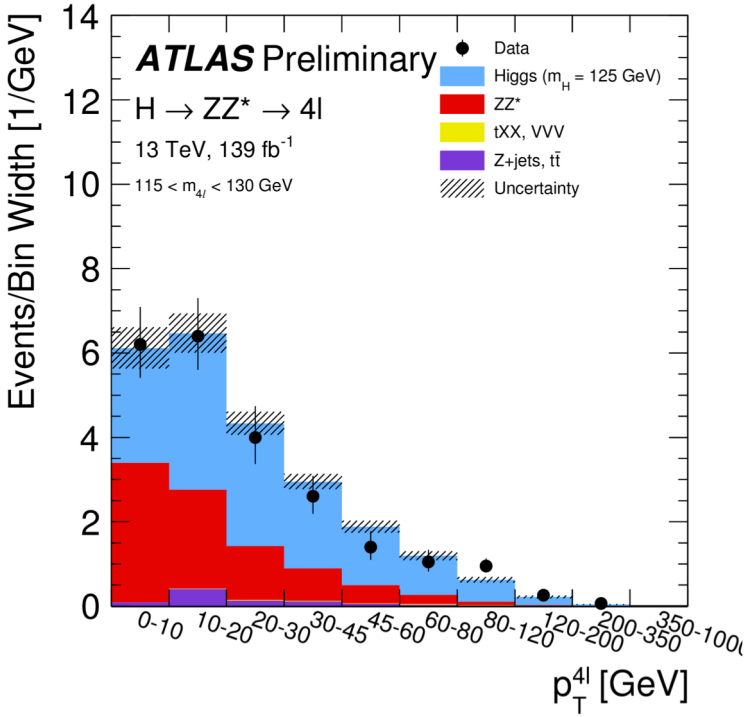

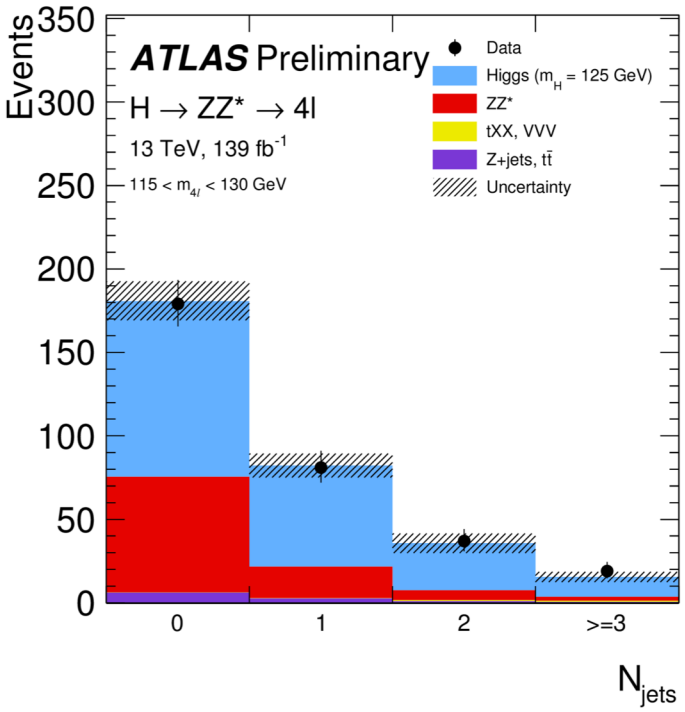

ZZ normalization factors are also obtained in bins of p_T^{4l} , N_{jets}

Cross section measurements

- Fiducial definition
  - Leptons (dressed): $p_T > 20, 15, 10, 5$ GeV, $|\eta| < 2.7$
  - Jets: anti-k_T4 jets with $p_T > 30$ GeV, $|y| < 4.4$
  - $m_{12} \in (50, 106)$ GeV, $m_{34} \in (12, 115)$ GeV
  - $m_{4l} \in (105, 160)$ GeV
  - (Details in the backup)
- Measured fiducial cross sections:
  - σ_{fid} = 3.35 ± 0.30 (stat.) ± 0.12 (syst.) fb
  - Still statistically limited
  - Consistent with SM prediction of 3.41 ± 0.18 fb, with *p*-value of 85%
- Unfolding
  - Response matrix method as the default
  - Cross checked with bin-by-bin correction factor method

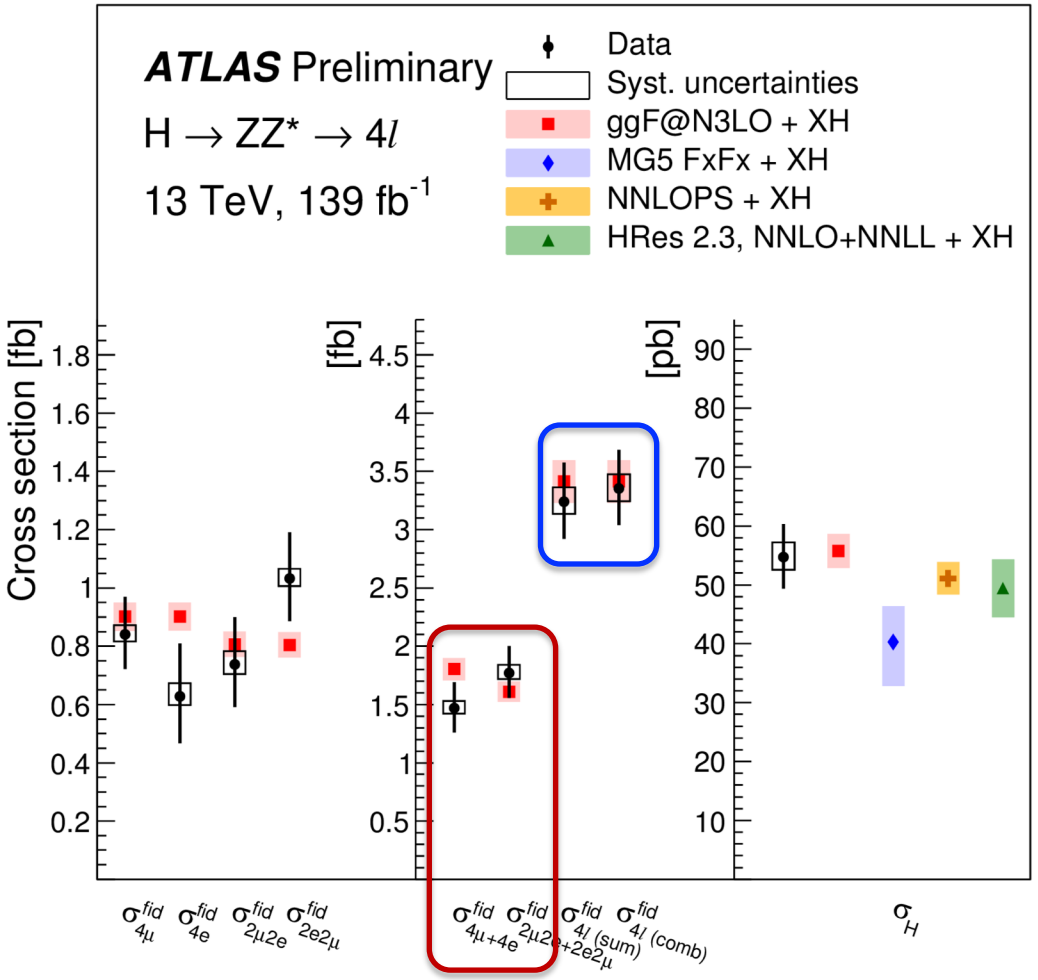

Same-flavor (4e, 4μ) cross sections probe the interference effects between the identical final state fermions(~10%)

Differential results: p_{T}^{4l}

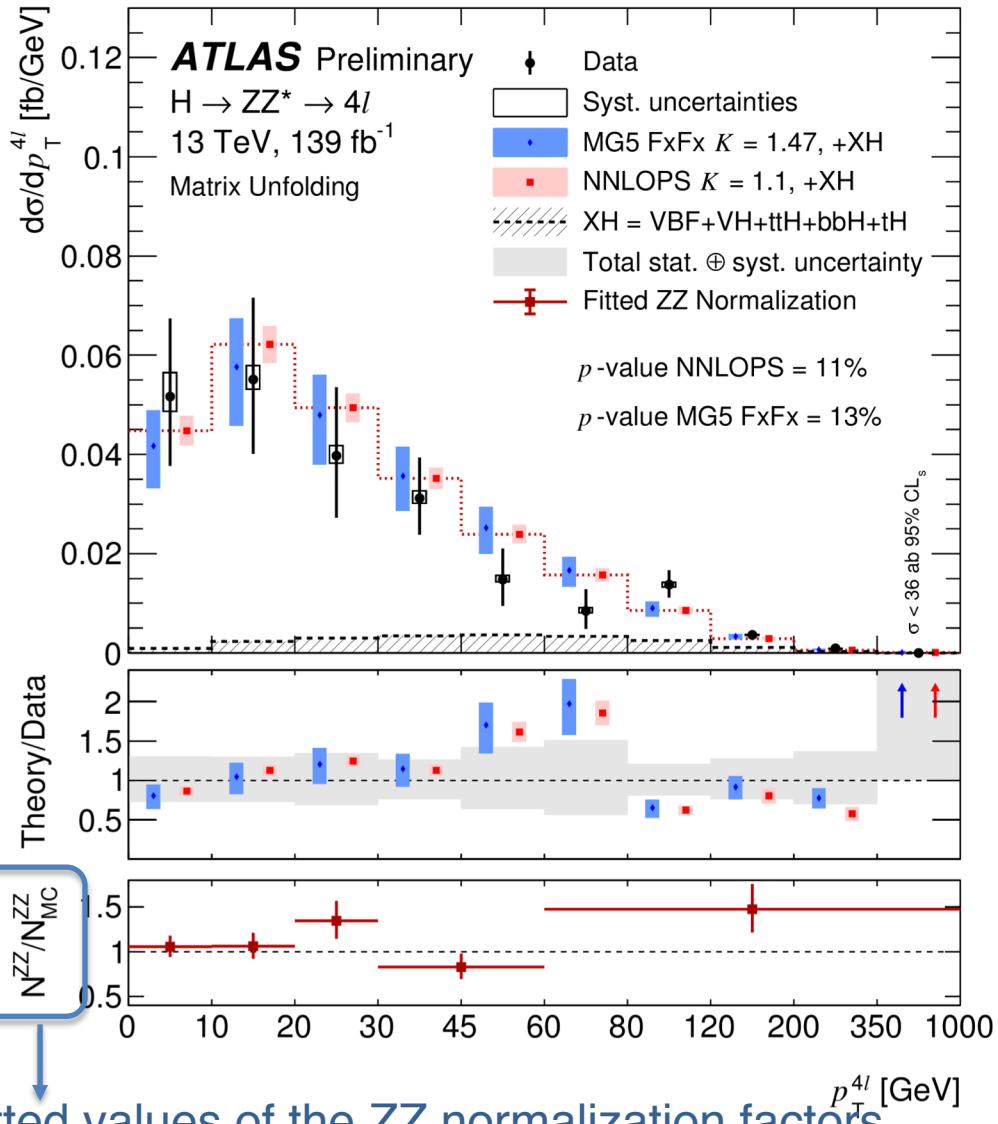

Fitted values of the ZZ normalization factors

Higgs p_T:

- Sensitive to perturbative QCD calculations
- Low p_T region sensitive to light quark Yukawa couplings
- High p_T region sensitive to potential new particles in ggF loop

ggF predictions by NNLOPS and MG5-FxFx are normalized to the N^{3}LO total cross section

Consistent with SM (NNLOPS) prediction: p-value 11%

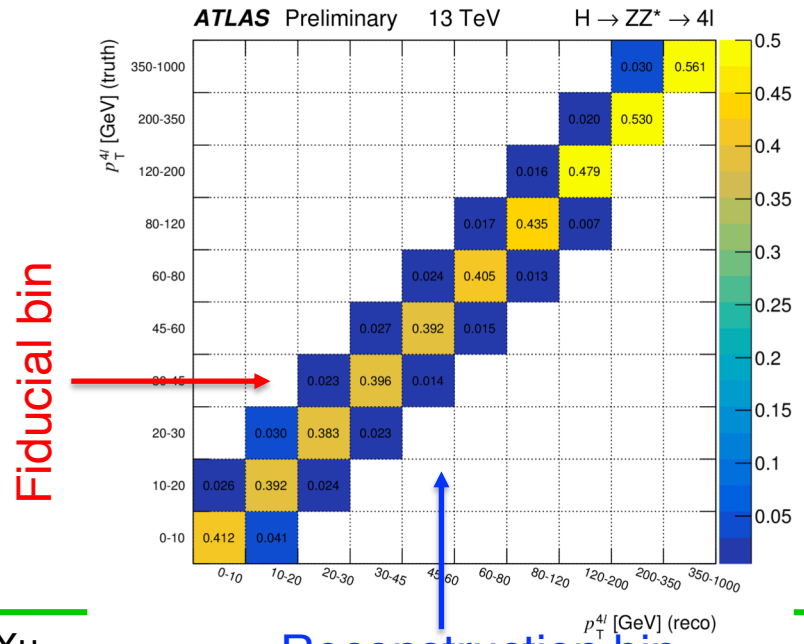

Response matrix

Differential results: N_{jets}

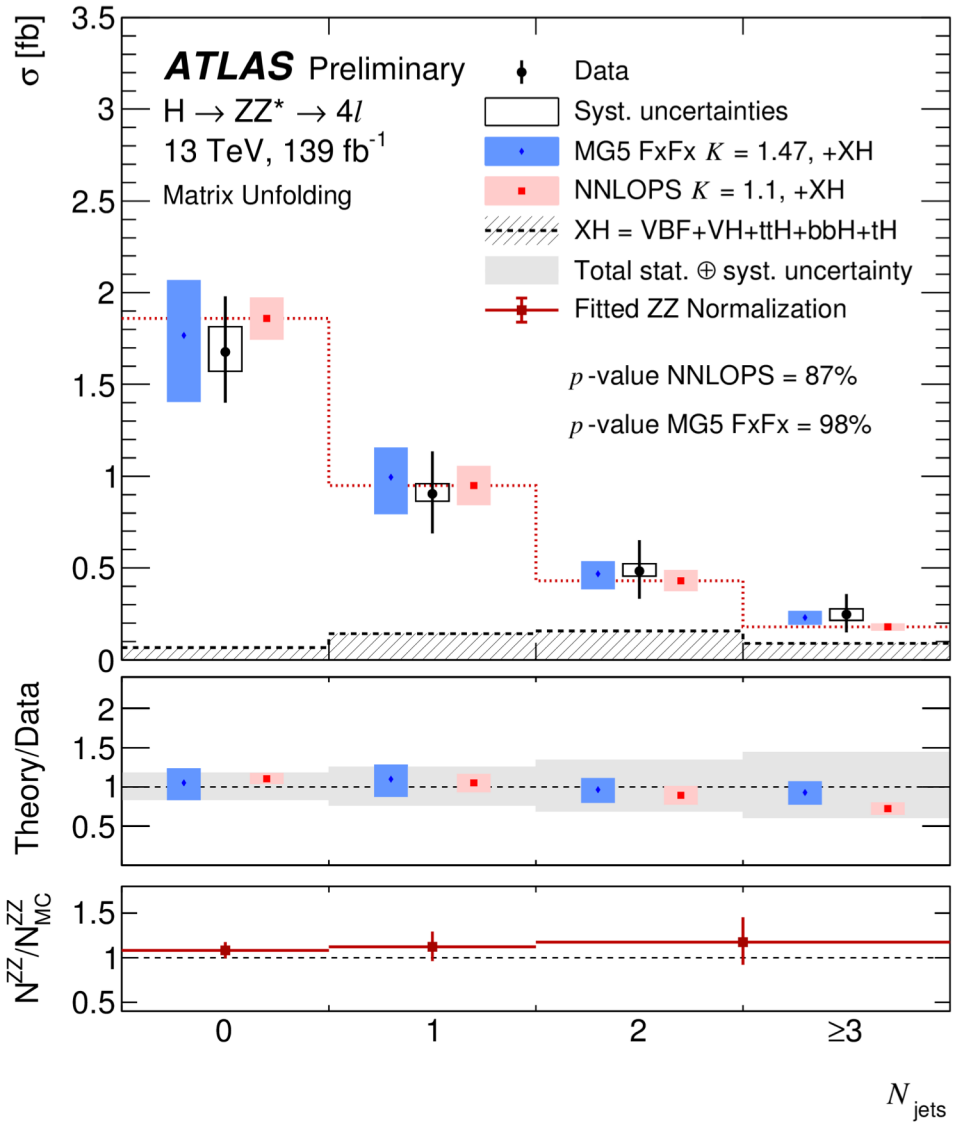

N_{jets}: sensitive to higher-order QCD calculations

ggF predictions by NNLOPS and MG5-FxFx are normalized to the N^3LO total cross section

Consistent with SM (NNLOPS) prediction: p-value 87%

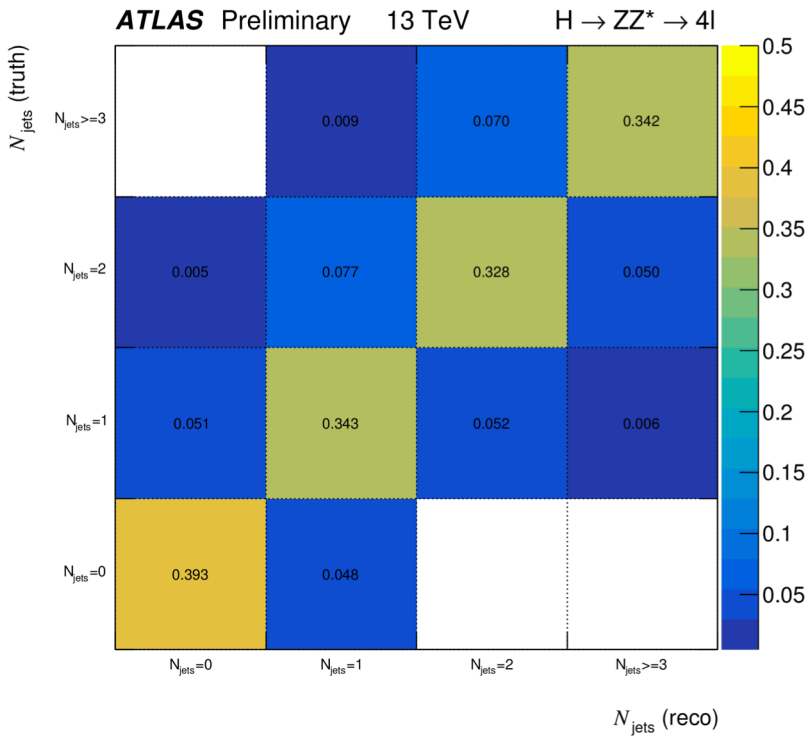

Response matrix

$H \rightarrow \gamma\gamma$

ATLAS-CONF-2019-029

Cross section measurements

- Fiducial definition:
  - γ: $p_T > 25$ GeV, $|\eta| < 2.37$ reject if $1.37 < |\eta| < 1.52$
  - Jets: anti-k_T4 jets with $p_T > 30$ GeV, $|y| < 4.4$
  - $m_{\gamma\gamma} \in (105, 160)$ GeV

- Measured fiducial cross sections:
  - σ_{fid} = 65.2 ± 4.5 (stat.) ± 5.6 (syst.) ± 0.3 (theo.) fb
  - Becoming systematic limited
    - Leading syst.: Background modelling and photon energy resolution
  - Consistent with SM prediction of 63.6 ± 3.3 fb

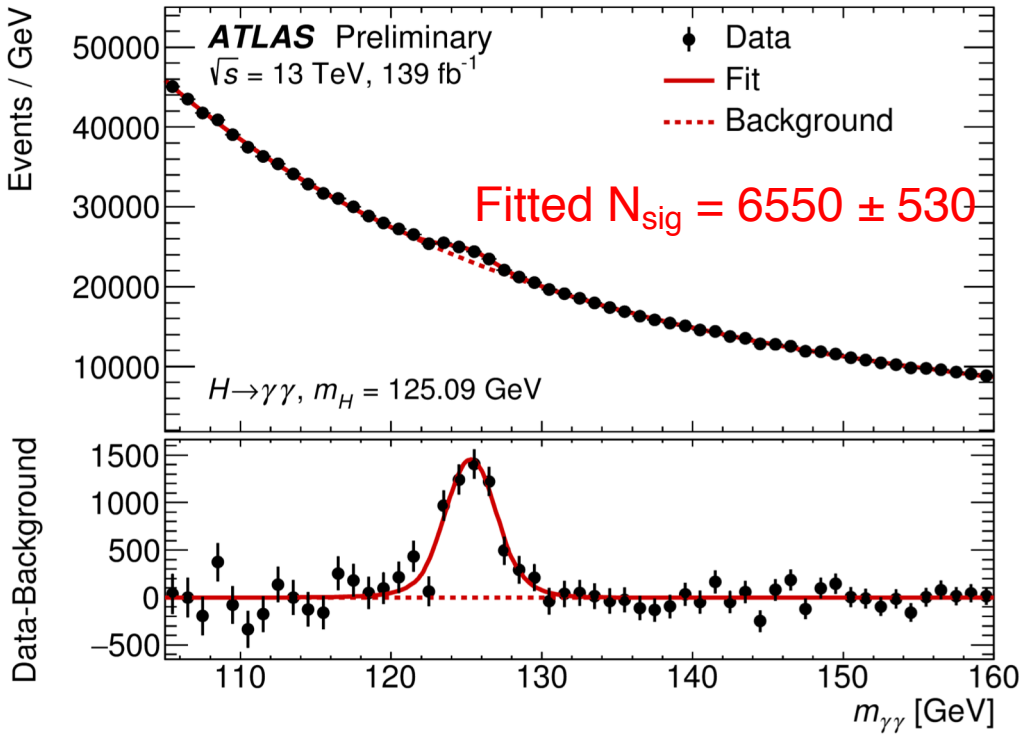

- Unfolding
  - Bin-by-bin correction factor unfolding as the default
  - Cross checked with response matrix method

$$\left(\frac{d\sigma}{dx}\right)_i = \frac{N_i^{sig}}{c_{fid,i}\,\Delta x_i\,\mathcal{L}_{int}}$$

Differential results: $p_T^{\gamma\gamma}$, $|y_{\gamma\gamma}|$

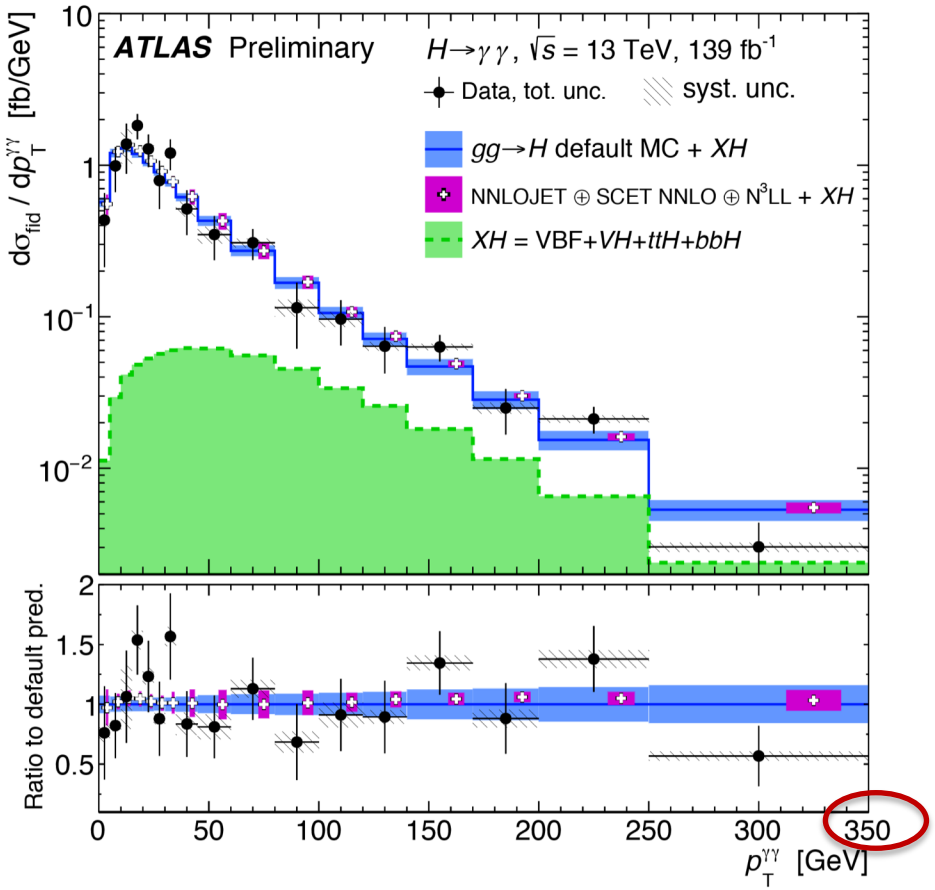

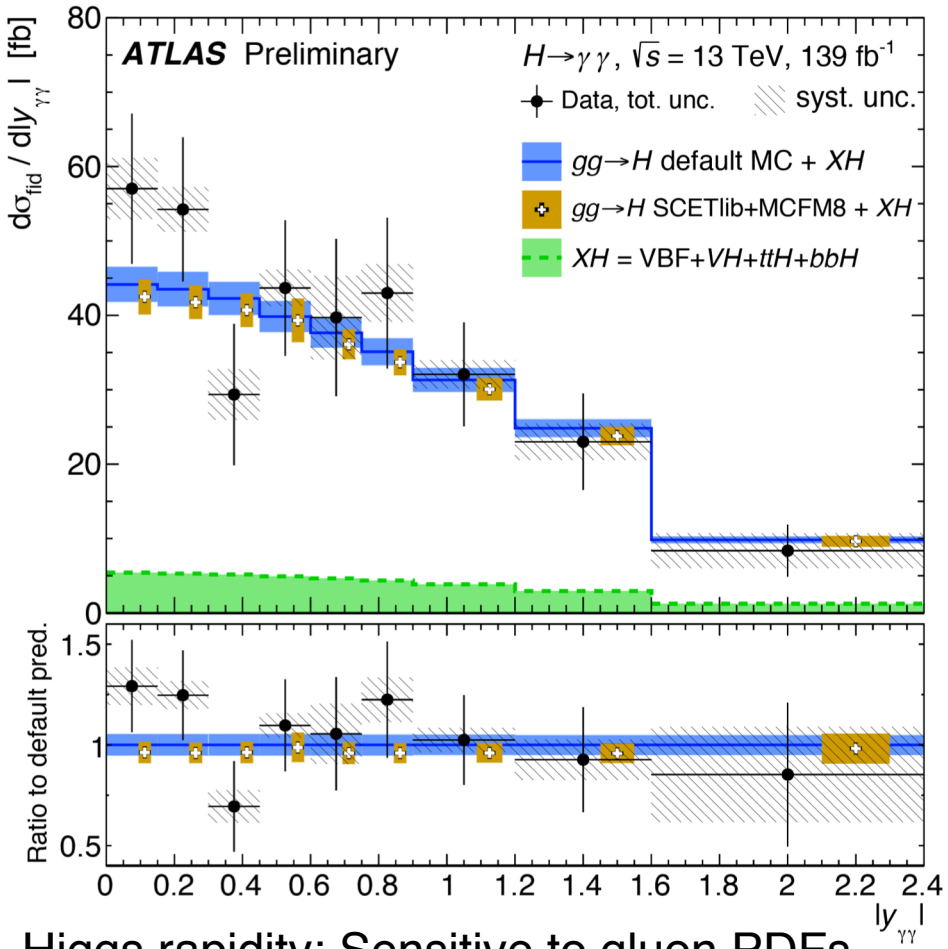

NNLOJET+SCET is more precise in the high p_T region

Higgs rapidity: Sensitive to gluon PDFs

Inclusive cross section for $p_T^{\gamma\gamma}$ > 350 GeV is measured to be 0.23 ± 0.14 fb, consistent with SM of 0.21 fb

SCETlib+MCFM8 provides predictions for $|y_{\gamma\gamma}|$ at NNLO+NNLL'$_\phi$ accuracy

Differential results: N_{jets}, $\Delta\phi_{jj}$

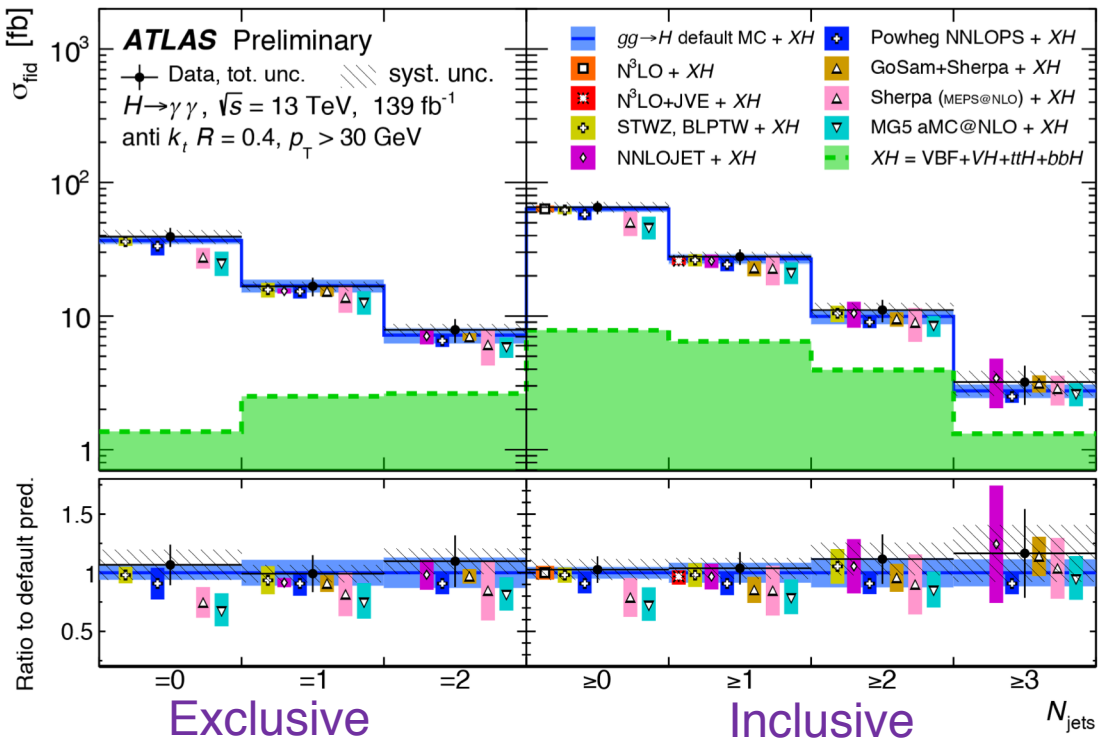

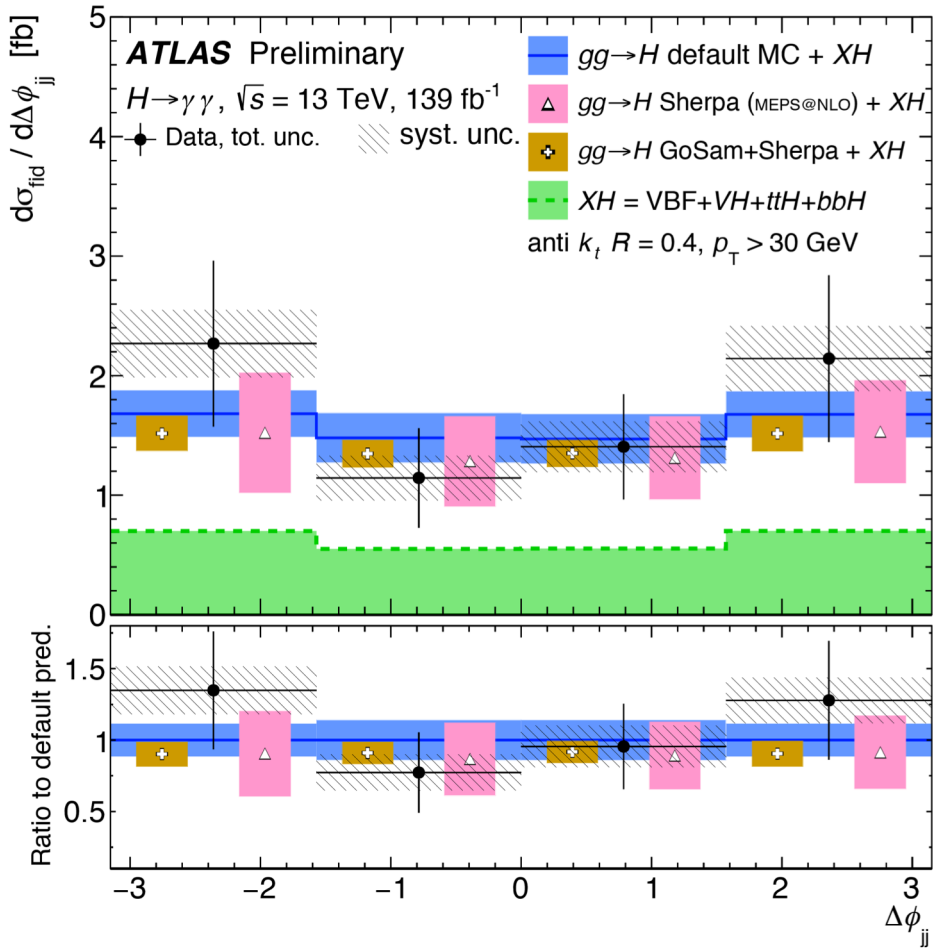

Compared to various predictions

Measured N_{jets} distribution consistent with all predictions with precision better than NLO

$\Delta\phi_{jj}$: sensitive to the CP properties of the Higgs boson

GoSam is more precise, with H+0,1,2,3j@NLO

Combination of $H \rightarrow ZZ^* \rightarrow 4l$ and $H \rightarrow \gamma\gamma$

ATLAS-CONF-2019-032

Combination

- The combined cross section is extracted for the total phase space
  - Introduce more model dependence and acceptance uncertainty
  - But significantly reduce measurement uncertainties → still limited by data statistics

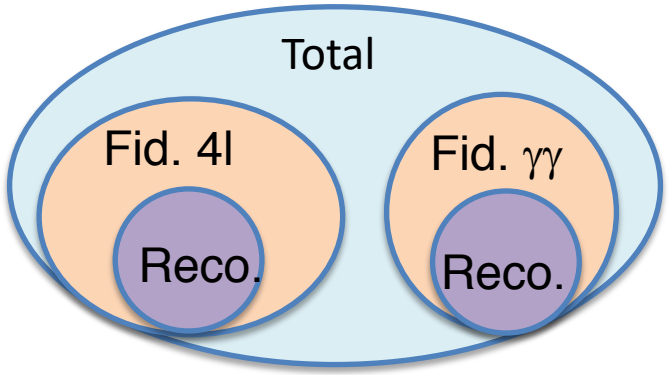

- Acceptance correction:
  - Extrapolate 4l and γγ to the total phase space
  - 4l: overall 49%; 45% at low $p_{T,H}$ to 65% at high $p_{T,H}$
  - γγ : overall 50%; 50% at low $p_{T,H}$, 45% at intermediate values, and about 75% at high $p_{T,H}$

- Unfolding: bin-by-bin correction factor
  - Only $p_{T,H}$ differential measurement is considered for the moment
  - Migration effect very small for $p_{T,H}$

Combined total cross section

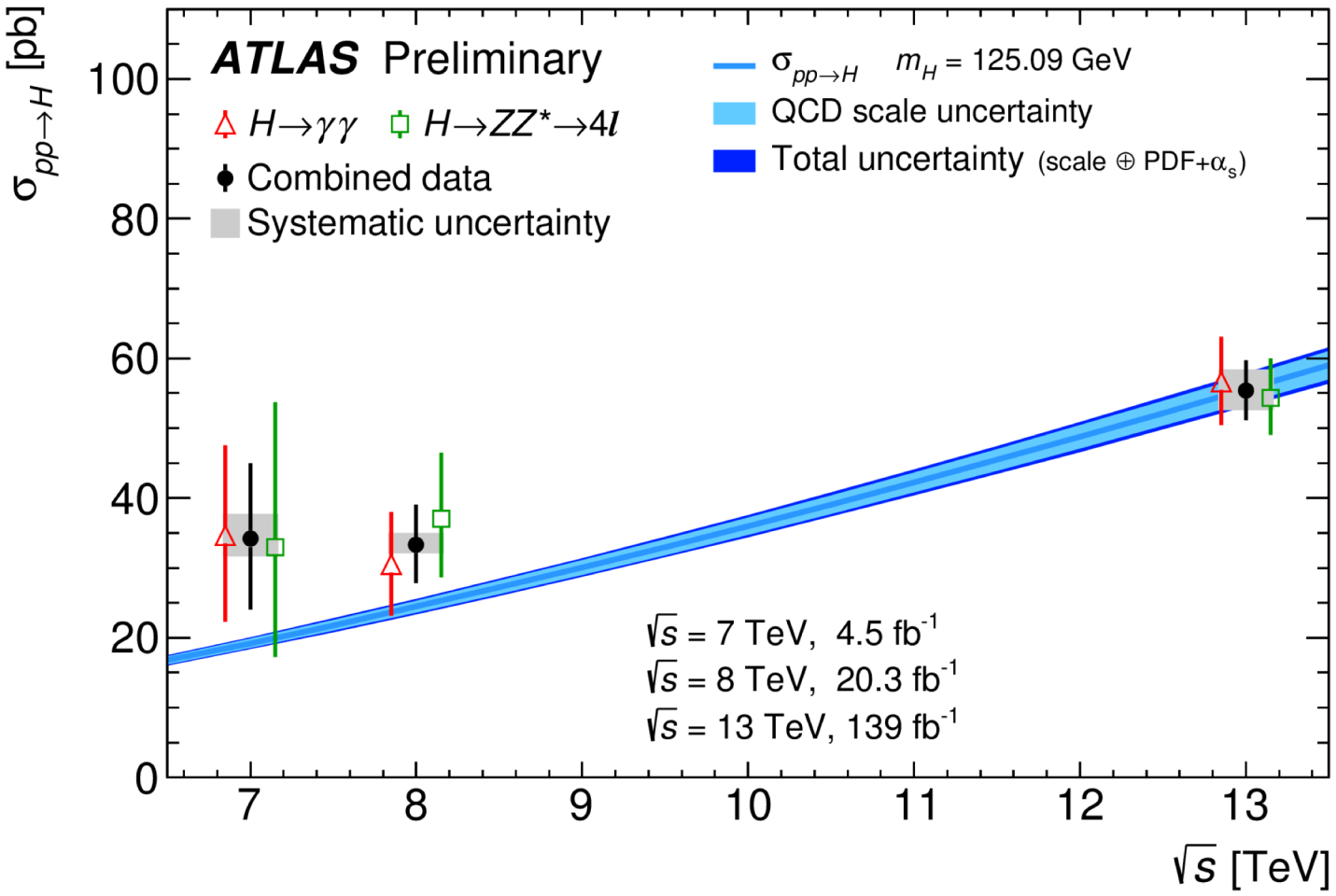

$\sigma_{pp\to H}$ [pb] at $\sqrt{s}$ =13 TeV	
H→ZZ*→4l	$54.4^{+5.6}_{-5.4}$
H→γγ	$56.7^{+6.4}_{-6.2}$
Combined	$55.4^{+4.3}_{-4.2}$ (±3.1(stat.) $^{+3.0}_{-2.8}$ (sys.))
SM prediction	**55.6 ± 2.5**

The two channels are compatible with a *p*-value of 76%

All three results are in agreement with the SM prediction

Combined differential results

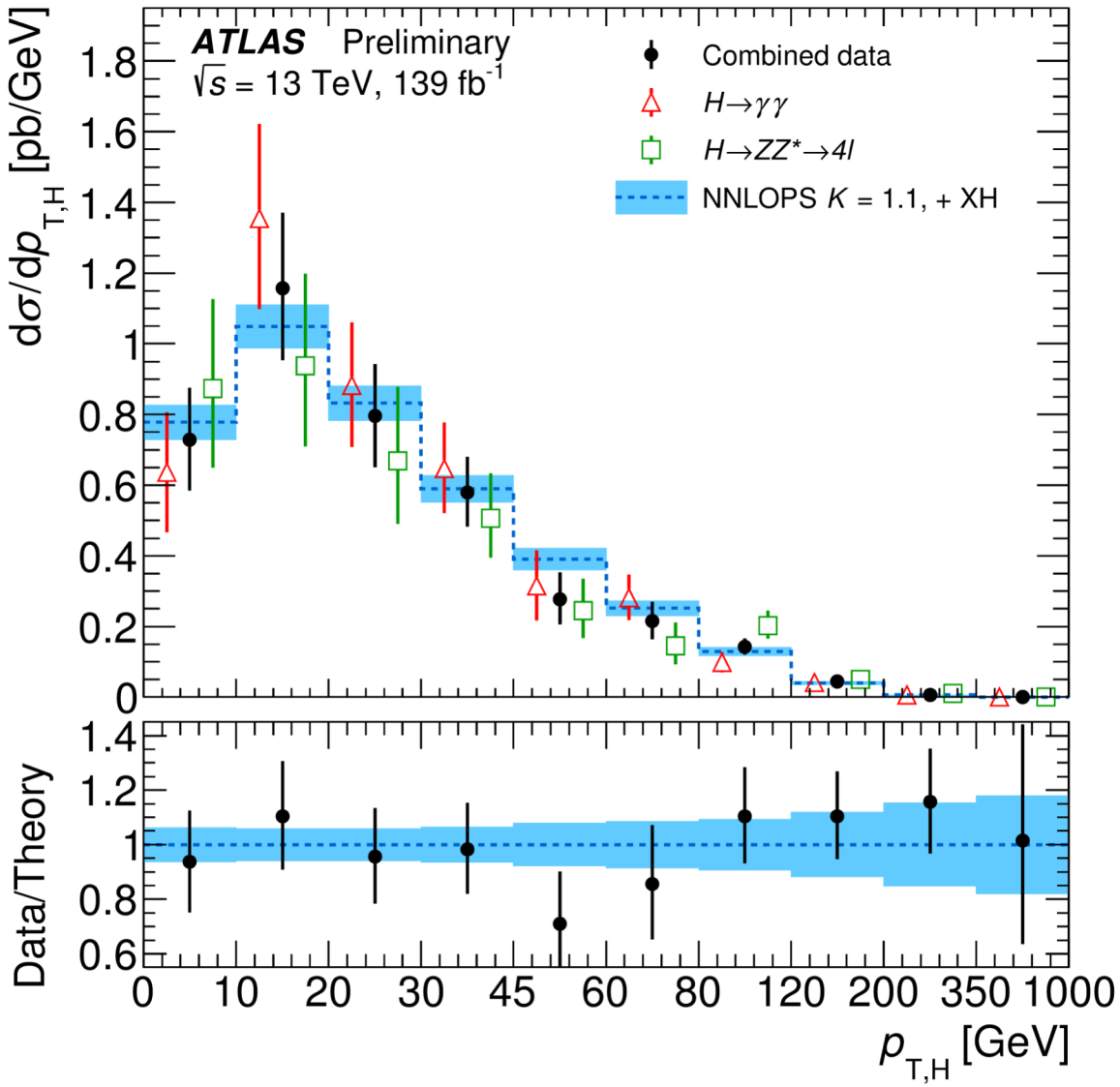

The measurement uncertainty is dominated by the statistical component

The two channels are compatible, with *p*-value of 11%

Compatible with SM, with *p*-value of 78%

Interpretations of Higgs differential measurements ($H \rightarrow \gamma\gamma$ only)

ATLAS-CONF-2019-029

EFT interpretation: this talk

Charm-quark Yukawa coupling: F. Braren's talk

EFT interpretation

- Probe new physics via an effective field theory approach
- Two EFT frameworks:
  - Higgs Effective Lagrangian in the Strongly Interacting Light Higgs basis (SILH)
  - SMEFT with Warsaw basis

$$\mathcal{L}_{\rm EFT} = \mathcal{L}_{\rm SM} + \sum_i \frac{c_i}{\Lambda^2} O_i^{(6)},$$

$$\mathcal{L}_{\rm eff}^{\rm SILH} \supset \bar{c}_g O_g + \bar{c}_\gamma O_\gamma + \bar{c}_{HW} O_{HW} + \bar{c}_{HB} O_{HB} + \tilde{c}_g \tilde{O}_g + \tilde{c}_\gamma \tilde{O}_\gamma + \tilde{c}_{HW} \tilde{O}_{HW} + \tilde{c}_{HB} \tilde{O}_{HB},$$

Modify Hgg and Hγγ couplings — Modify HVV couplings

$$\mathcal{L}_{\rm eff}^{\rm SMEFT} \supset \bar{C}_{HG} O'_g + \bar{C}_{HW} O'_{HW} + \bar{C}_{HB} O'_{HB} + \bar{C}_{HWB} O'_{HWB} + \tilde{C}_{HG} \tilde{O}'_g + \tilde{C}_{HW} \tilde{O}'_{HW} + \tilde{C}_{HB} \tilde{O}'_{HB} + \tilde{C}_{HWB} \tilde{O}'_{HWB},$$

Modify ggF production — Modify VBF/VH production and Hγγ decay

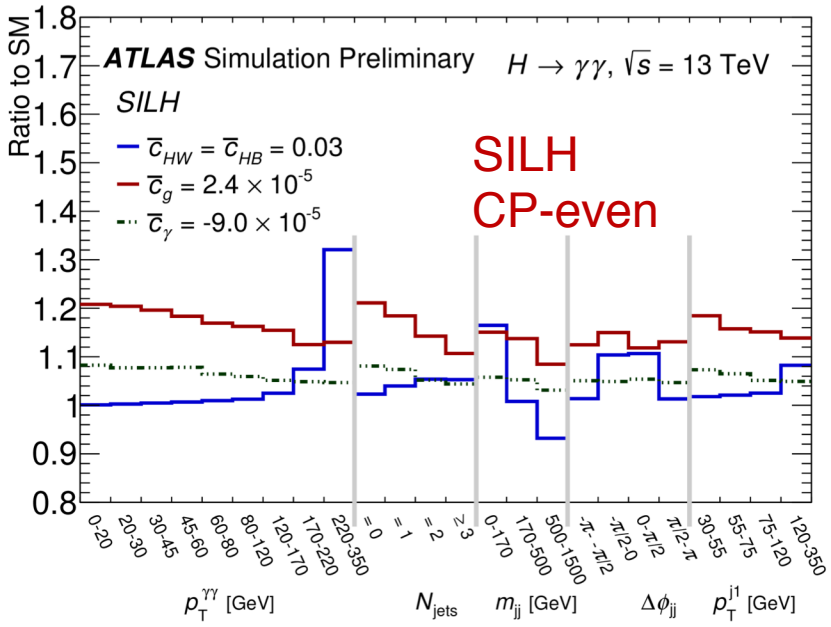

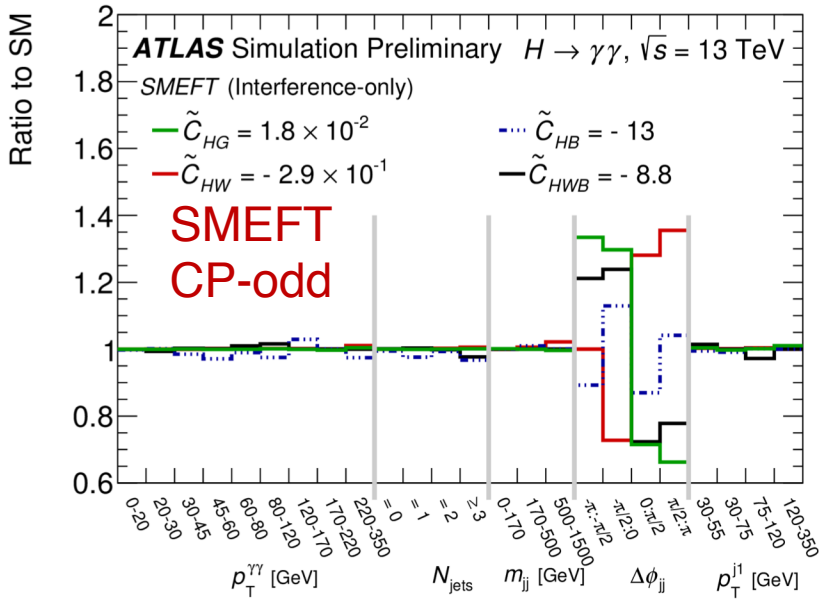

Statistical interpretation

- Construct a likelihood using 5 unfolded observables to constrain Wilson coefficients
  - $p_T^{\gamma\gamma}$, N_{jets}, p_T^{j1}, m_{jj}, $\Delta\phi_{jj}$

$$\mathcal{L} = \frac{1}{\sqrt{(2\pi)^k\,|C|}} \exp\left(-\frac{1}{2}\left(\vec{\sigma}_{\text{data}} - \vec{\sigma}_{\text{pred}}\right)^T C^{-1}\left(\vec{\sigma}_{\text{data}} - \vec{\sigma}_{\text{pred}}\right)\right),$$

  - Covariance matrix: $C = C_{stat} + C_{syst} + C_{theo}$
  - σ_{data}: unfolded differential measurements
  - σ_{pred}: parton-level events MadGraph5+Pythia8
    - Assumption: higher-order QCD and EW corrections are the same for SM and BSM
    - "K-factors" obtained from SM are applied to BSM

$$\frac{d\sigma}{dX} = \sum_j \left(\frac{d\sigma_j}{dX}\right)^{\text{ref}} \cdot \left(\frac{d\sigma_j}{dX}\right)^{\text{MG5}}_{c_i} \Big/ \left(\frac{d\sigma_j}{dX}\right)^{\text{MG5}}_{c_i=0},$$

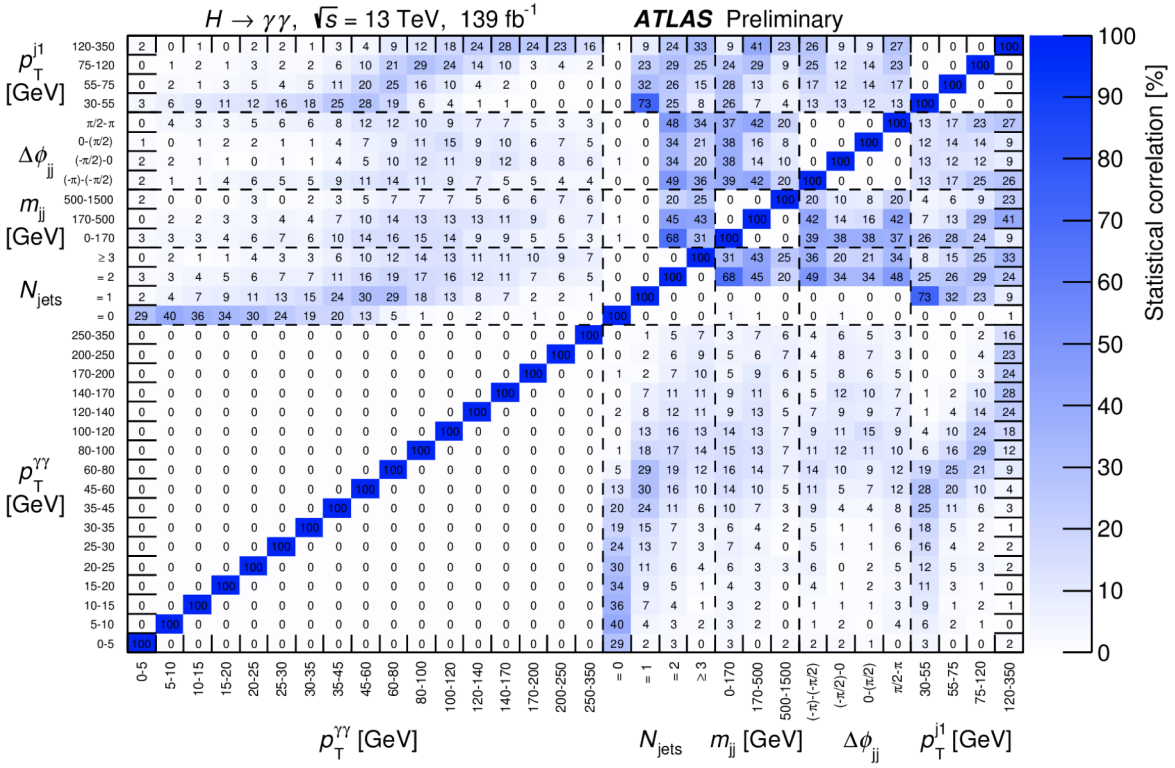

Results

- Results presented for both SILH and SMEFT formulations
  - SILH: both 1D and 2D limits

SILH

Coefficient	Observed 95% CL limit
$\bar{c}_g$	$[-0.26, 0.26] \times 10^{-4}$
$\tilde{c}_g$	$[-1.3, 1.1] \times 10^{-4}$
$\bar{c}_{HW}$	$[-2.5, 2.2] \times 10^{-2}$
$\tilde{c}_{HW}$	$[-6.5, 6.3] \times 10^{-2}$
$\bar{c}_\gamma$	$[-1.1, 1.1] \times 10^{-4}$
$\tilde{c}_\gamma$	$[-2.8, 4.3] \times 10^{-4}$

About a factor 2 improvement compared to the 36 fb^{-1} results

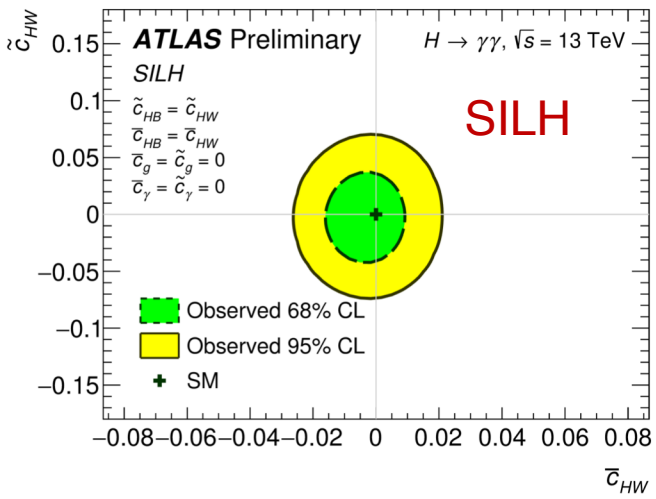

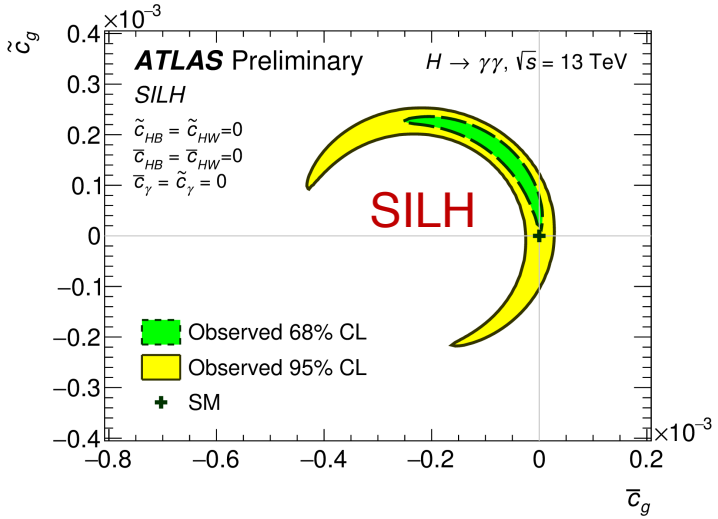

SMEFT, interference-only term Interference + quadratic

  - SMEFT: two scenarios
    - Only the interference term considered
    - Interference + quadratic terms

$$\sigma \propto |\mathcal{M}_{\rm EFT}|^2 = |\mathcal{M}_{\rm SM}|^2 + |\mathcal{M}_{\rm d6}|^2 + 2Re(\mathcal{M}^*_{\rm SM}\mathcal{M}_{\rm d6}) \ ,$$

Coefficient	95% CL, interference-only terms	95% CL, interference and quadratic terms
$\bar{C}_{HG}$	$[-4.2, 4.8] \times 10^{-4}$	$[-6.1, 4.7] \times 10^{-4}$
$\tilde{C}_{HG}$	$[-2.1, 1.6] \times 10^{-2}$	$[-1.5, 1.4] \times 10^{-3}$
$\bar{C}_{HW}$	$[-8, 2, 7.4] \times 10^{-4}$	$[-8.3, 8.3] \times 10^{-4}$
$\tilde{C}_{HW}$	$[-0.26, 0.33]$	$[-3.7, 3.7] \times 10^{-3}$
$\bar{C}_{HB}$	$[-2.4, 2.3] \times 10^{-4}$	$[-2.4, 2.4] \times 10^{-4}$
$\tilde{C}_{HB}$	$[-13.0, 14.0]$	$[-1.2, 1.1] \times 10^{-3}$
$\bar{C}_{HWB}$	$[-4.0, 4.4] \times 10^{-4}$	$[-4.2, 4.2] \times 10^{-4}$
$\tilde{C}_{HWB}$	$[-11.1, 6.5]$	$[-2.0, 2.0] \times 10^{-3}$

Summary

- Latest results on Higgs fiducial and differential measurements with full run 2 data:
  - $H \rightarrow ZZ^* \rightarrow 4l$ and $H \rightarrow \gamma\gamma$ channels, and the combination
  - Results improved: increased luminosity, improved analysis techniques
  - Fiducial cross section in $H \rightarrow \gamma\gamma$ becomes systematically limited
  - Differential measurements still statistically limited
  - Measurements are all consistent with SM predictions

- Interpretations in the context of Effective Field Theory:
  - Using 5 differential observables in $H \rightarrow \gamma\gamma$ to probe the tensor structure of the Higgs boson interactions
  - Improved limits with SILH basis (a factor of two)
  - First limits on the SMEFT basis

- More results are coming:
  - Other channels, more differential observables, interpretations etc.

Backup

Fiducial phase space: H→ZZ*→4l

Leptons and jets	
Leptons	$p_T > 5$ GeV, $\|\eta\| < 2.7$
Jets	$p_T > 30$ GeV, $\|y\| < 4.4$
remove jets with	$\Delta R(\text{jet}, \ell) < 0.1$
Lepton selection and pairing	
Lepton kinematics	$p_T > 20, 15, 10$ GeV
Leading pair (m_{12})	SFOS lepton pair with smallest $\|m_Z - m_{\ell\ell}\|$
Subleading pair (m_{34})	remaining SFOS lepton pair with smallest $\|m_Z - m_{\ell\ell}\|$
Event selection (at most one quadruplet per event)	
Mass requirements	50 GeV$< m_{12} <$ 106 GeV and 12 GeV $< m_{34} <$ 115 GeV
Lepton separation	$\Delta R(\ell_i, \ell_j) > 0.1$
J/ψ veto	$m(\ell_i, \ell_j) > 5$ GeV for all SFOS lepton pairs
Mass window	105 GeV $< m_{4\ell} <$ 160 GeV
If extra leptons with $p_T > 12$ GeV	Quadruplet with the largest ME

Response matrix method

- Response matrix unfolding

The number of expected events N_i in each observable reconstruction bin *i:*

$$N_i(m_{4\ell}) = \sum_j r_{ij} \cdot (1 + f_i^{\text{nonfid}}) \cdot \sigma_j^{\text{fid}} \cdot \mathcal{P}(m_{4\ell}) \cdot \mathcal{L} + N_i^{bkg}(m_{4\ell})$$

Response matrix

Leakage from outside the fiducial region

Signal m4l template

i: reconstruction bin
j: fiducial bin

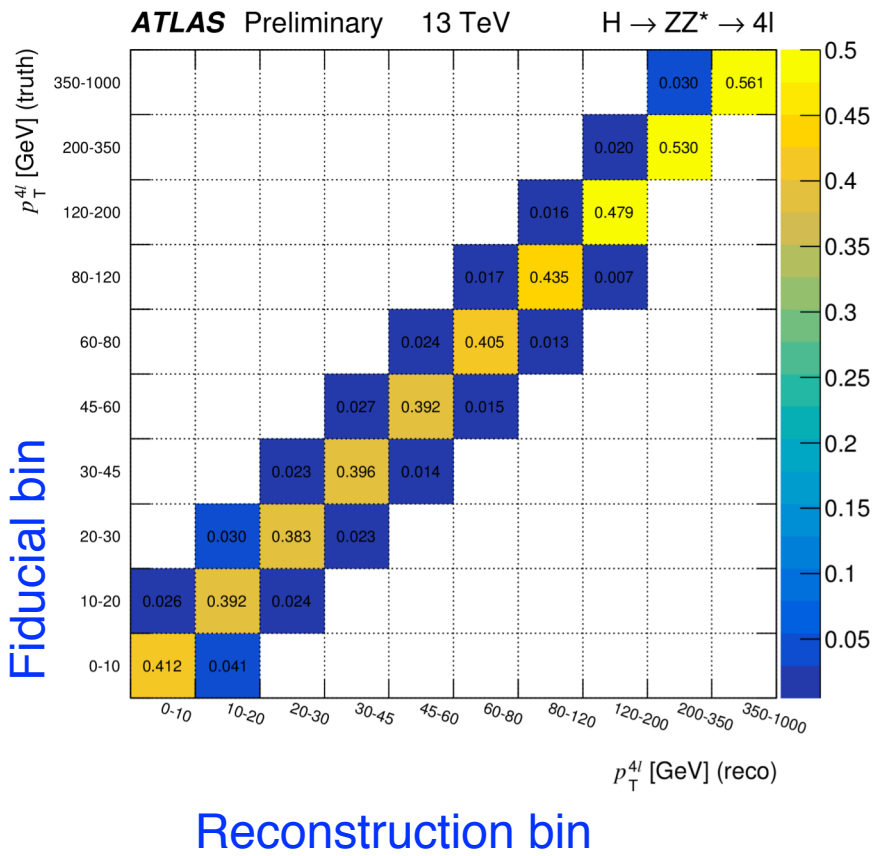

Fiducial bin

Reconstruction bin

Correlation matrix

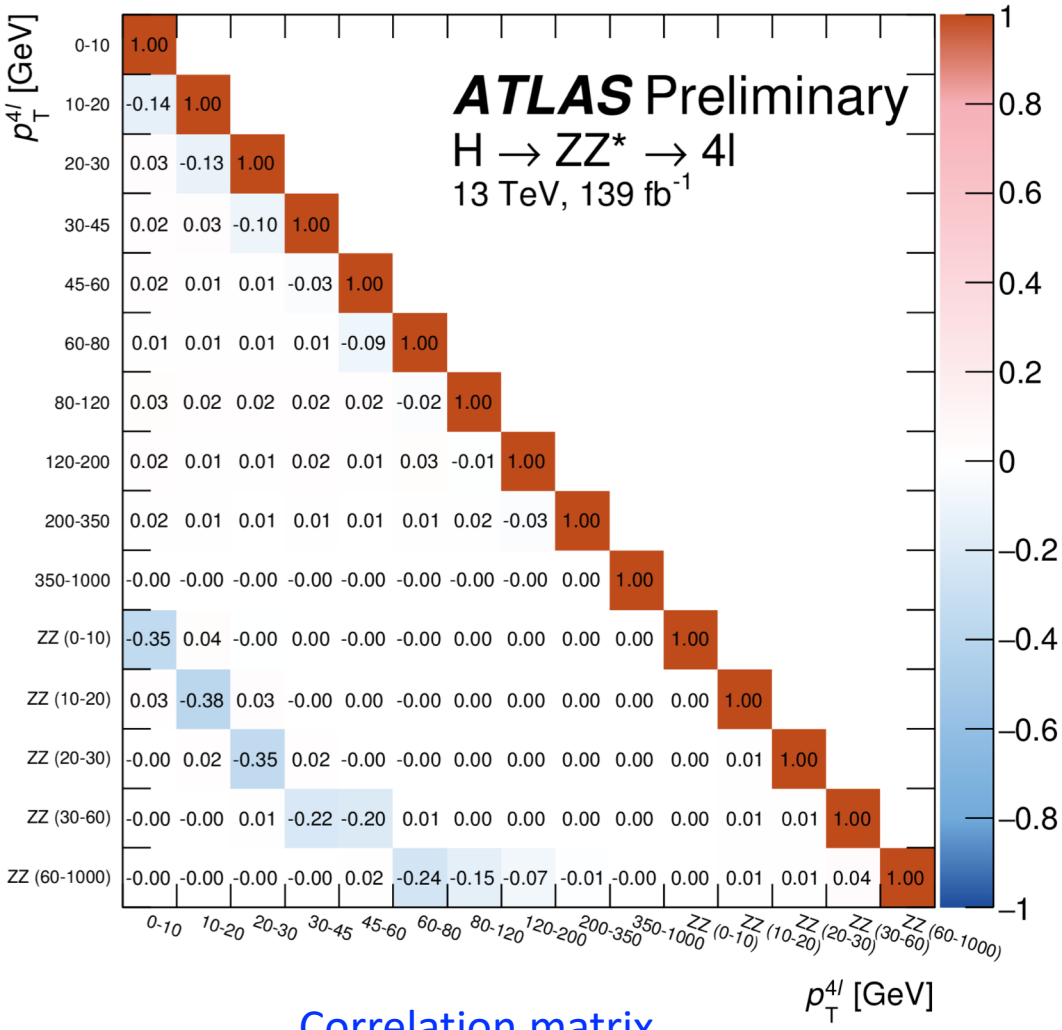

Correlation matrix

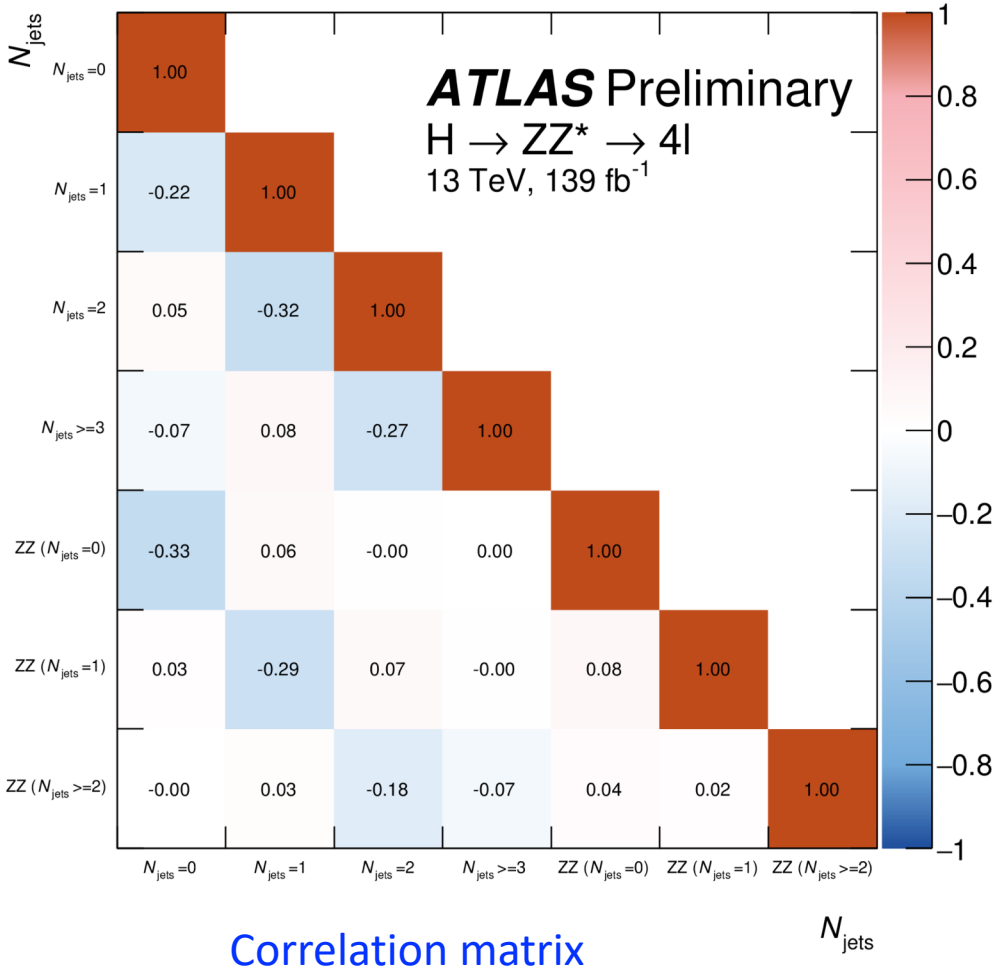

Correlation matrix

Response matrix vs bin-by-bin correction

- Unfolded p_{T}^{4l}

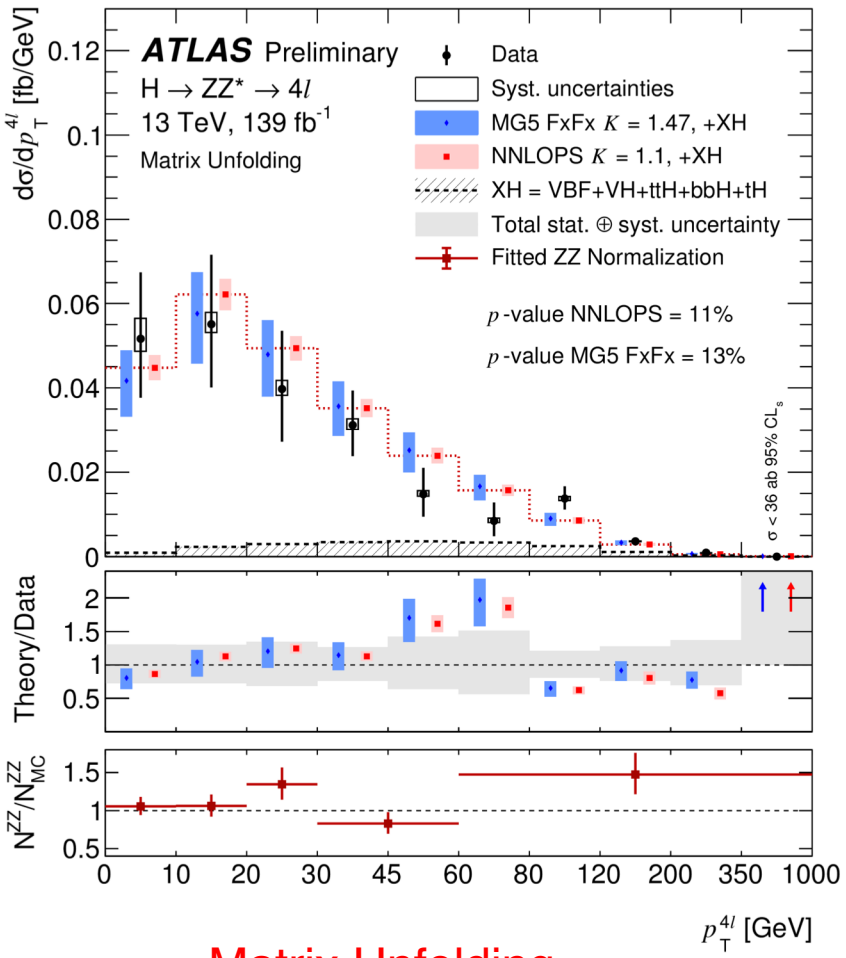

Matrix Unfolding

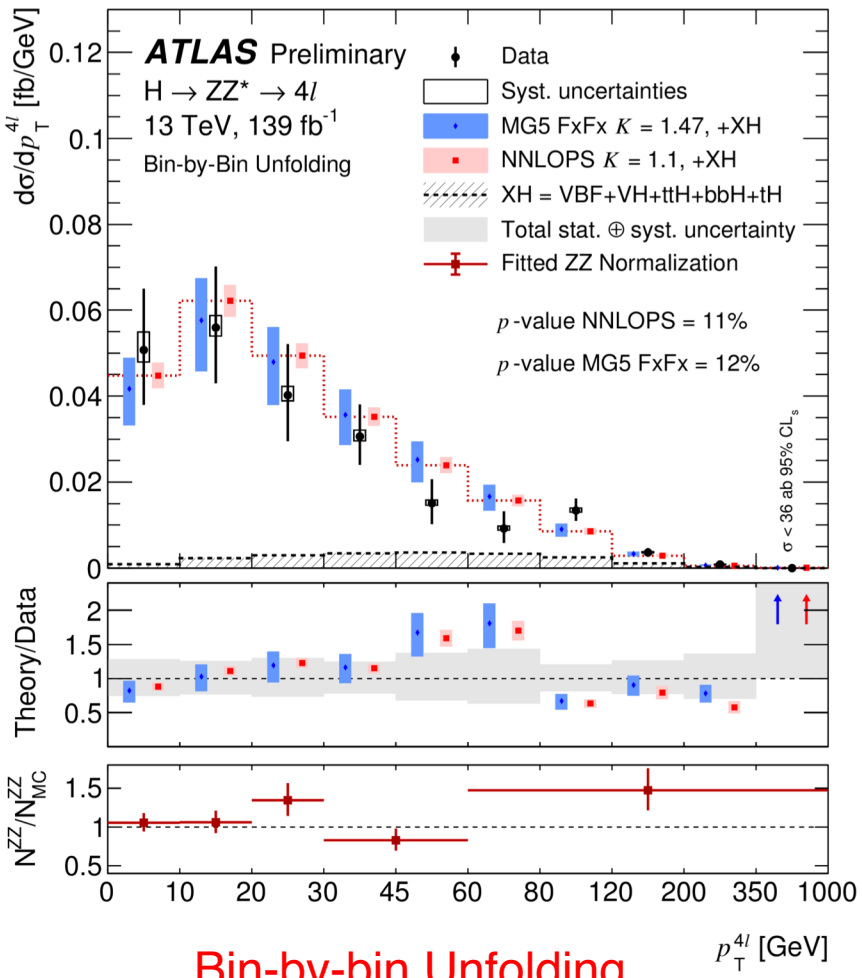

Bin-by-bin Unfolding

Response matrix vs bin-by-bin correction

- Unfolded N_{jets}

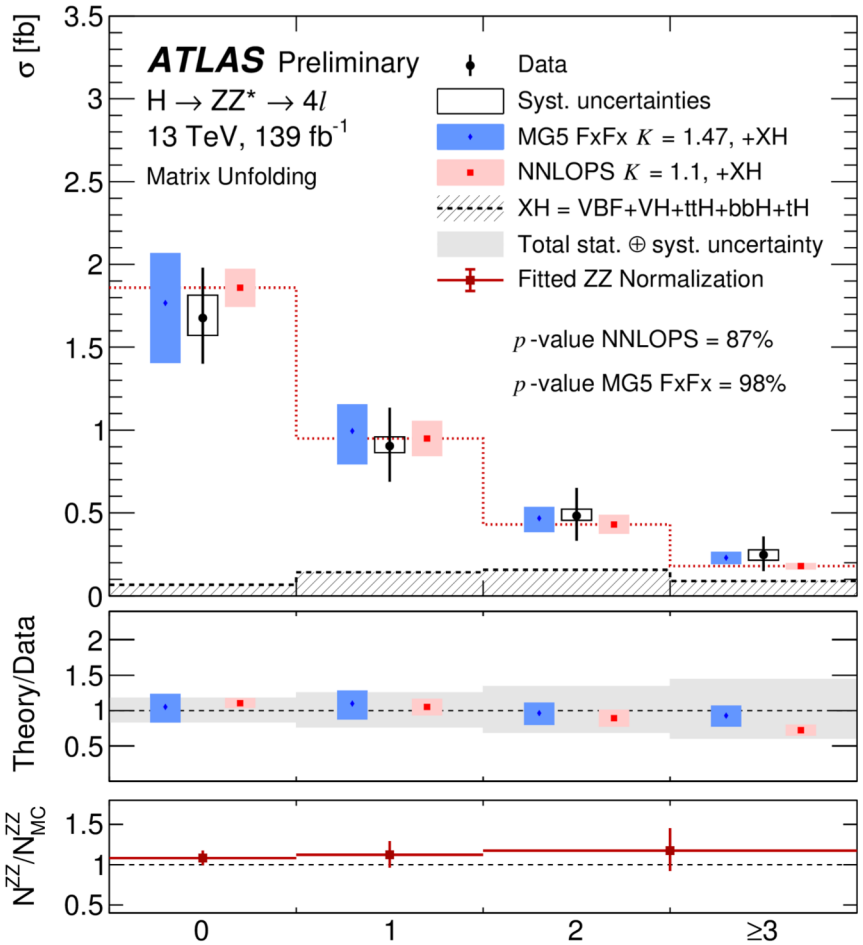

Matrix Unfolding

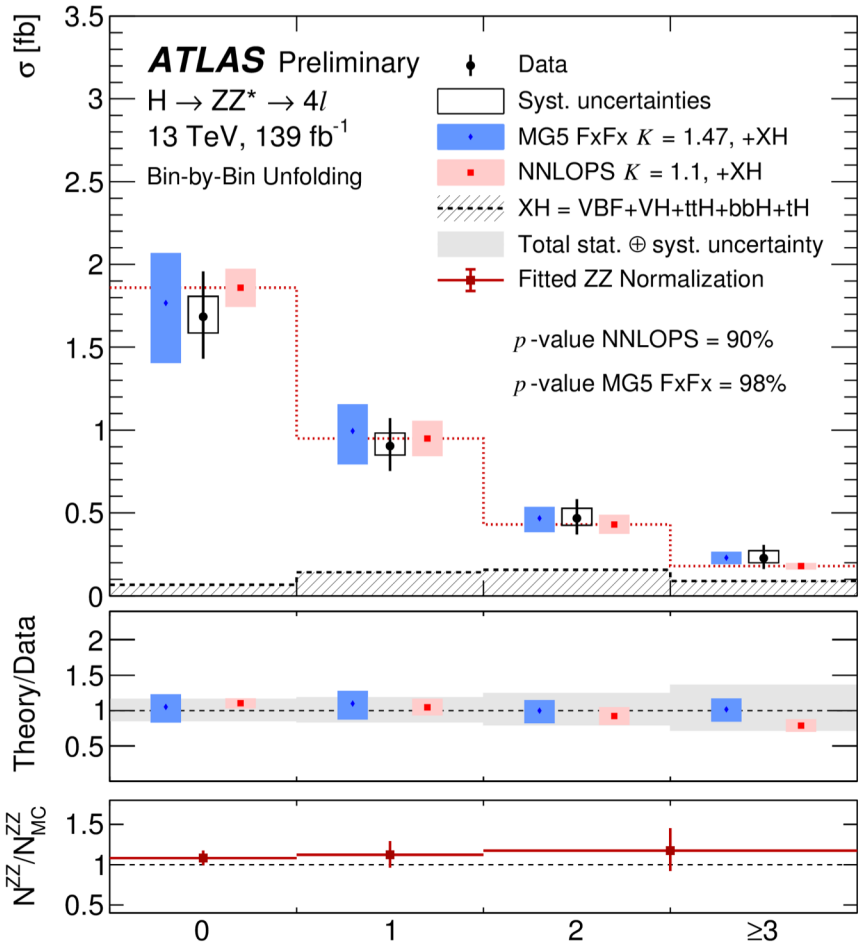

Bin-by-bin Unfolding

Systematic uncertainties: 4l

Measurement	Experimental uncertainties [%]				Theory uncertainties [%]					
	Lum.	e, μ, pile-up	Jets, flavour tagging	Reducible backgr.	ZZ^* backgr	tXX backgr.	Signal PDF	Signal QCD scale	Signal Parton Shower	Signal Composition
Fiducial cross section										
σ_{comb}	1.7	2.5	–	< 0.5	1	< 0.5	< 0.5	2	1	< 0.5
Per decay final state fiducial cross sections										
4μ	1.7	2.5	–	0.5	1	< 0.5	< 0.5	2	1	< 0.5
$4e$	1.7	7	–	0.5	1.5	< 0.5	< 0.5	2	0.5	< 0.5
$2\mu 2e$	1.7	5.5	–	0.5	1	< 0.5	< 0.5	2	1.5	< 0.5
$2e2\mu$	1.7	2.0	–	0.5	1	< 0.5	< 0.5	2	1	< 0.5
Stage-0 production bin cross sections										
ggF	1.7	1.5	1	0.5	1.5	< 0.5	0.5	1	2	–
VBF	1.7	1	4.5	0.5	2	0.5	1.5	8	6	–
VH	1.8	1.5	3.5	1	5	0.5	2	12	8	–
ttH	1.7	1	4.5	1	1	0.5	0.5	8	4	–

Fiducial phase space: H→γγ

Objects	Fiducial definition
Photons	$\lvert\eta\rvert < 2.37$ (excluding $1.37 < \lvert\eta\rvert < 1.52$), $\sum p_{\mathrm{T}}^{i}/p_{\mathrm{T}}^{\gamma} < 0.05$
Jets	anti-k_t, $R = 0.4$, $p_{\mathrm{T}} > 30$ GeV, $\lvert y\rvert < 4.4$
Diphoton	$N_\gamma \geq 2$, $105\,GeV < m_{\gamma\gamma} < 160\,GeV$, $p_{\mathrm{T}}^{\gamma_1}/m_{\gamma\gamma} > 0.35$, $p_{\mathrm{T}}^{\gamma_2}/m_{\gamma\gamma} > 0.25$

$\Delta\phi_{jj}$:
calculated from the two leading jets in the event as the difference in azimuthal angle between the more forward jet minus that of the more central one.

Systematic uncertainties: H→γγ

Source	Uncertainty (%)
Statistics	6.9
Signal extraction syst.	7.9
Photon energy scale & resolution	4.6
Background modelling (spurious signal)	6.4
Correction factor	2.6
Pile-up modelling	2.0
Photon identification efficiency	1.2
Photon isolation efficiency	1.1
Trigger efficiency	0.5
Theoretical modelling	0.5
Photon energy scale & resolution	0.1
Luminosity	1.7
Total	11.0

Unfolding uncertainties: H→γγ

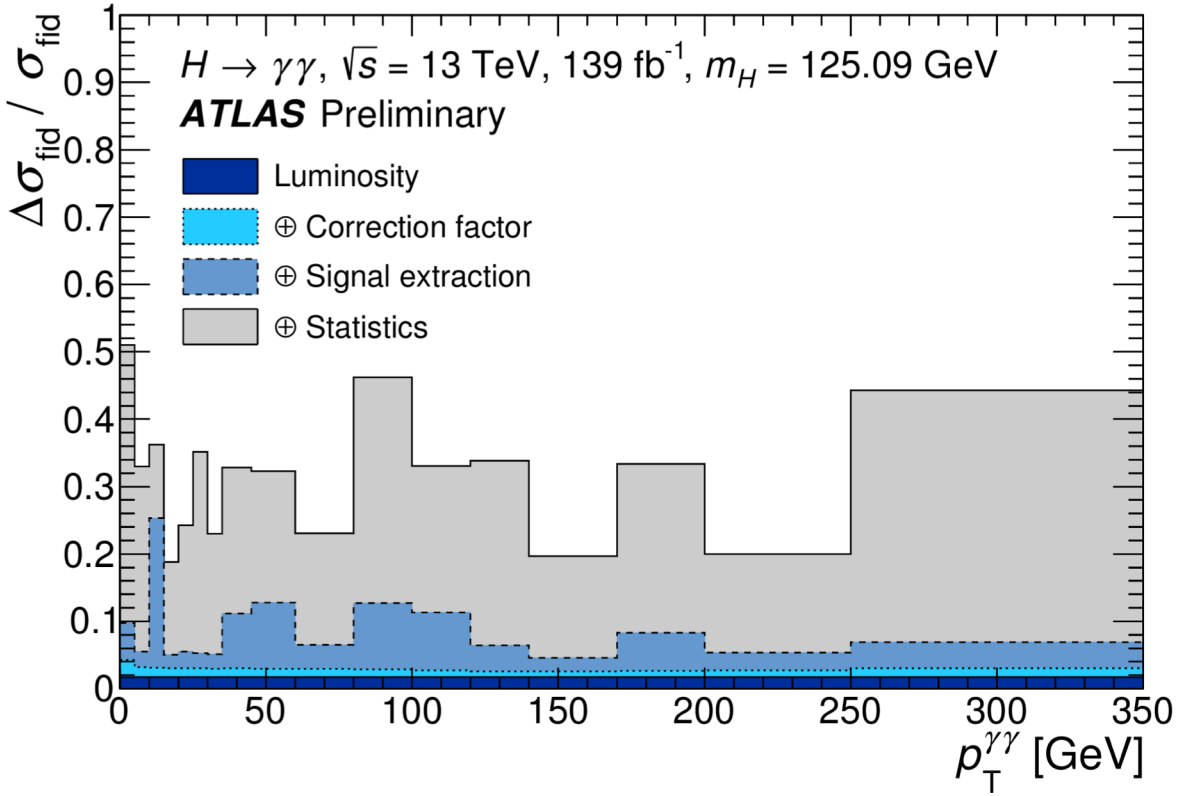

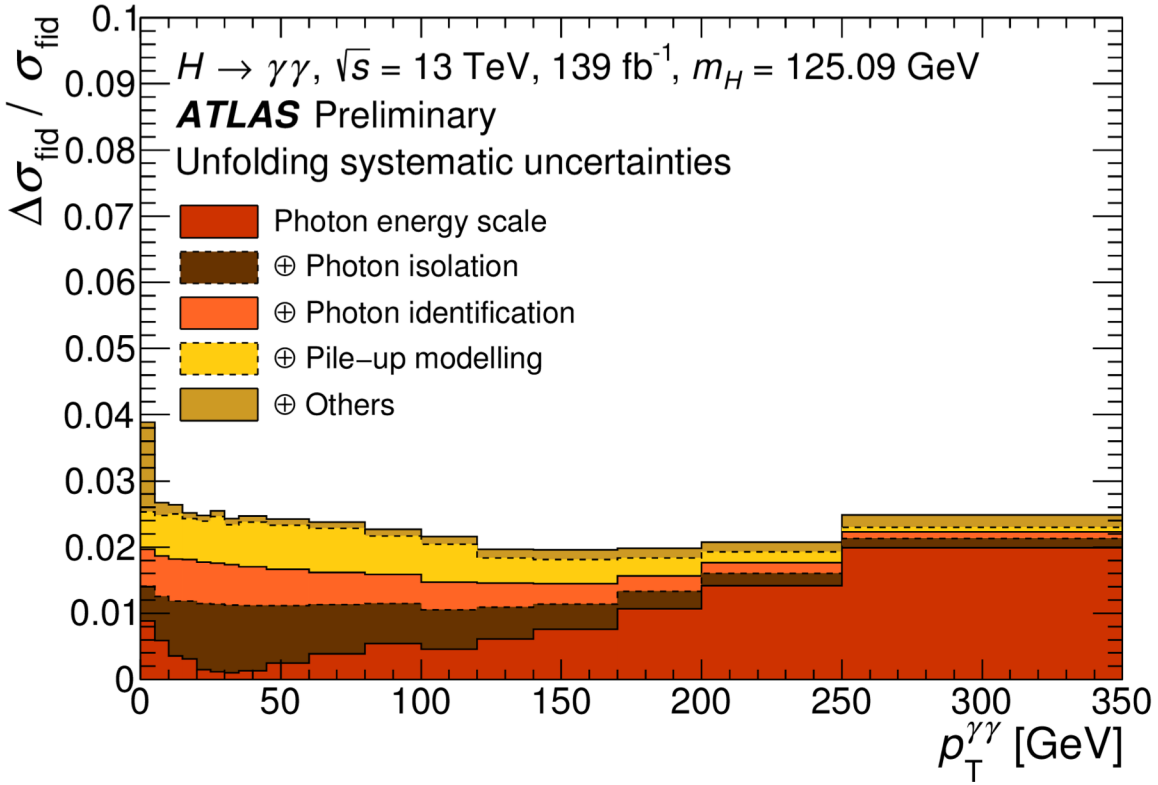

Statistical and systematic uncertainties relative to the differential cross sections measured in data, sequentially summed in quadrature, in each bin of the $p_T^{\gamma\gamma}$

The systematic uncertainties of the unfolding correction factors, sequentially summed in quadrature, in each bin of the $p_T^{\gamma\gamma}$

Differential results: p_T^{j1}, m_{jj}

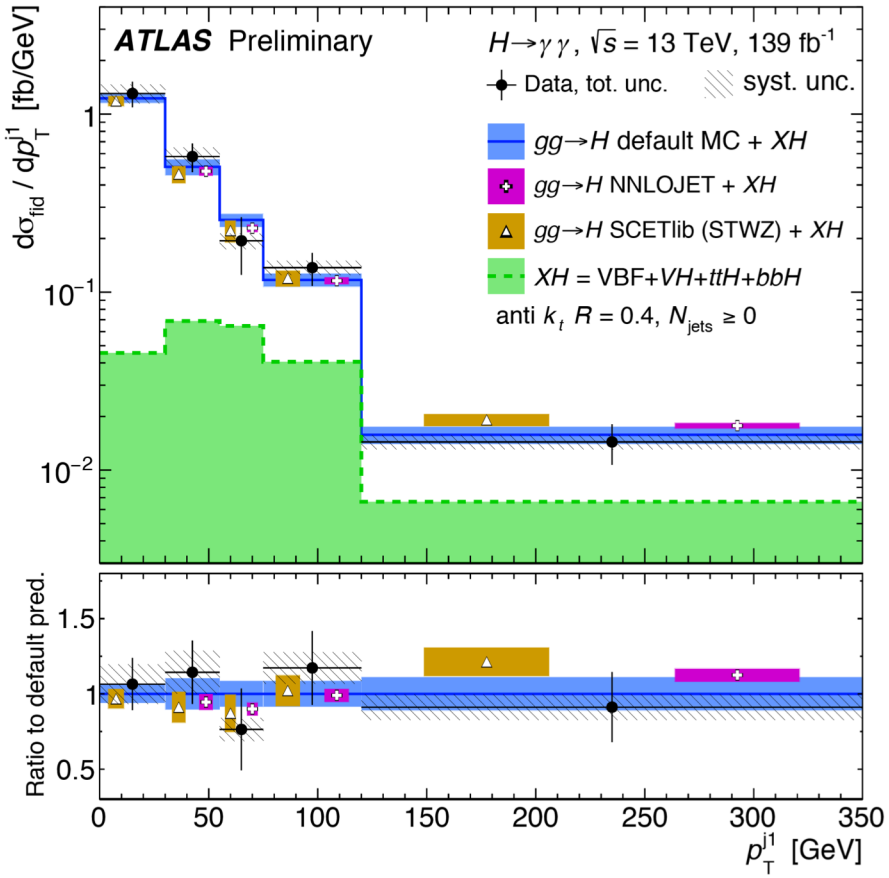

p_T^{j1}: probes the perturbative QCD prediction, sensitive to the relative contributions of the different Higgs production mechanisms.

NNLOJET is more precise in the high p_T^{j1} region.

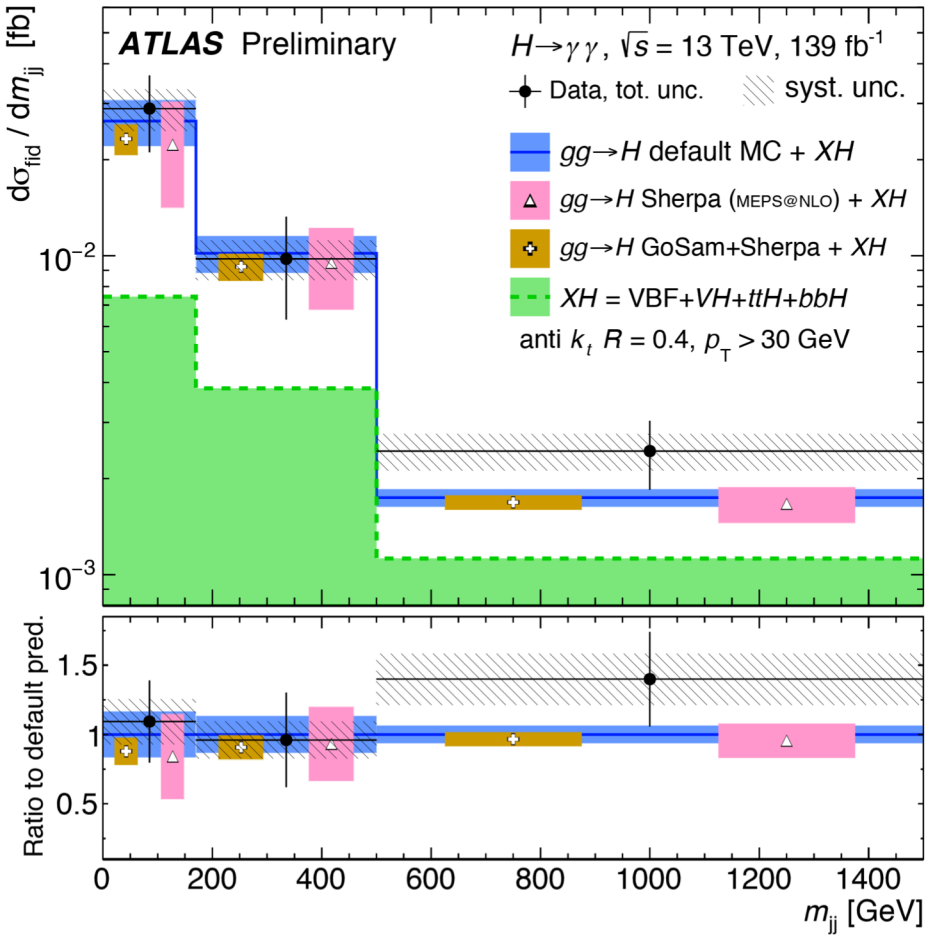

Higher m_{jj} bin sensitive to VBF production

GoSam is more precise, with H+0,1,2,3j@NLO

Theory predictions

- NNLOJET:
  - fixed-order NNLO prediction in QCD for inclusive H + 1-jet production.
- NNLOJET+SCET:
  - with N^3LL resummation matched to an NNLO fixed-order calculation in the heavy top-quark mass limit
- JVE+N^3LO:
  - includes NNLL resummation in QCD of the p_T of the leading jet which is matched to the N^3LO total cross section, shown only for the inclusive one-jet cross section.
- STWZ-BLPTW:
  - include NNLL0+NNLO resummation for the p_T of the leading jet in QCD, combined with a NLL0+NLO resummation in QCD for the subleading jet
- GoSam:
  - provides the fixed-order loop contributions accurate at NLO in QCD in the inclusive H + zero-jet, H + one-jet, H + two-jet, and H + three-jet regions. The real-emission contributions at fixed order in QCD are provided by Sherpa
- Sherpa (MEPS@NLO):
  - accurate to NLO in QCD in the inclusive H + zero-jet, H + one-jet, H + two-jet, and H + three-jet regions and includes top-quark mass effects
- SCETlib(STWZ):
  - provides predictions for p_{T}^{j1} at NNLL'+$NNLO_0$ accuracy by applying a resummation in p_{T}^{j1} .

EFT

SILH
CP-odd

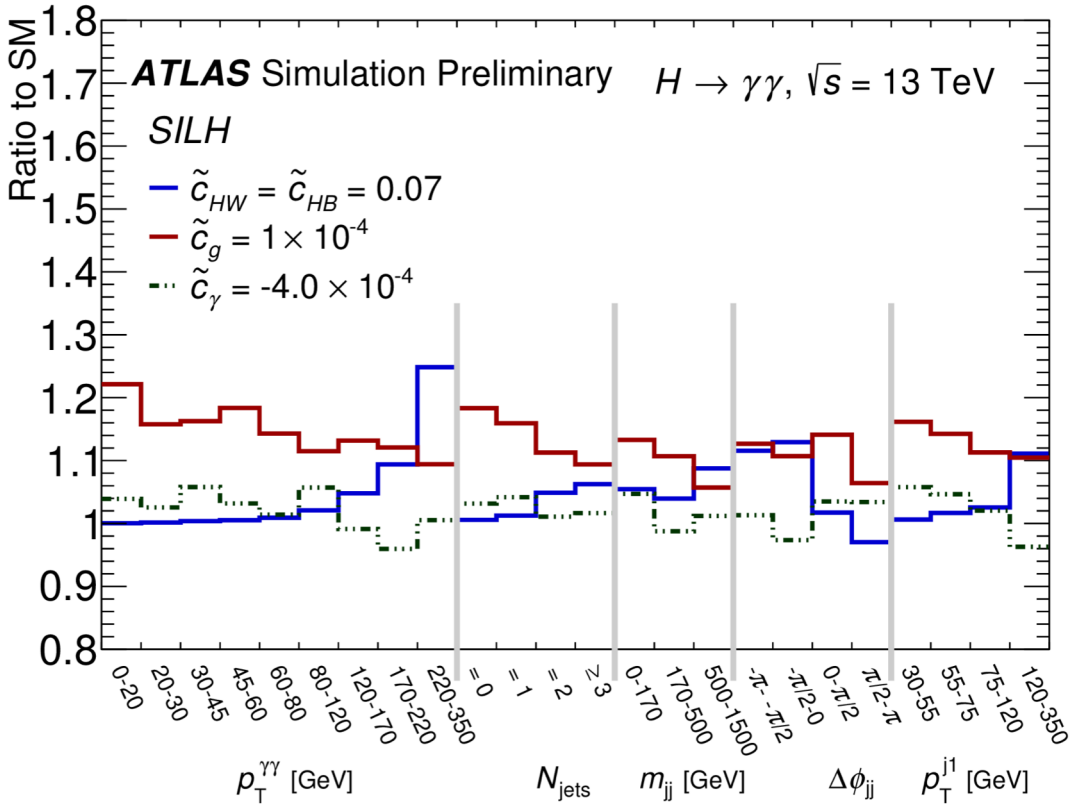

SMEFT
CP-even

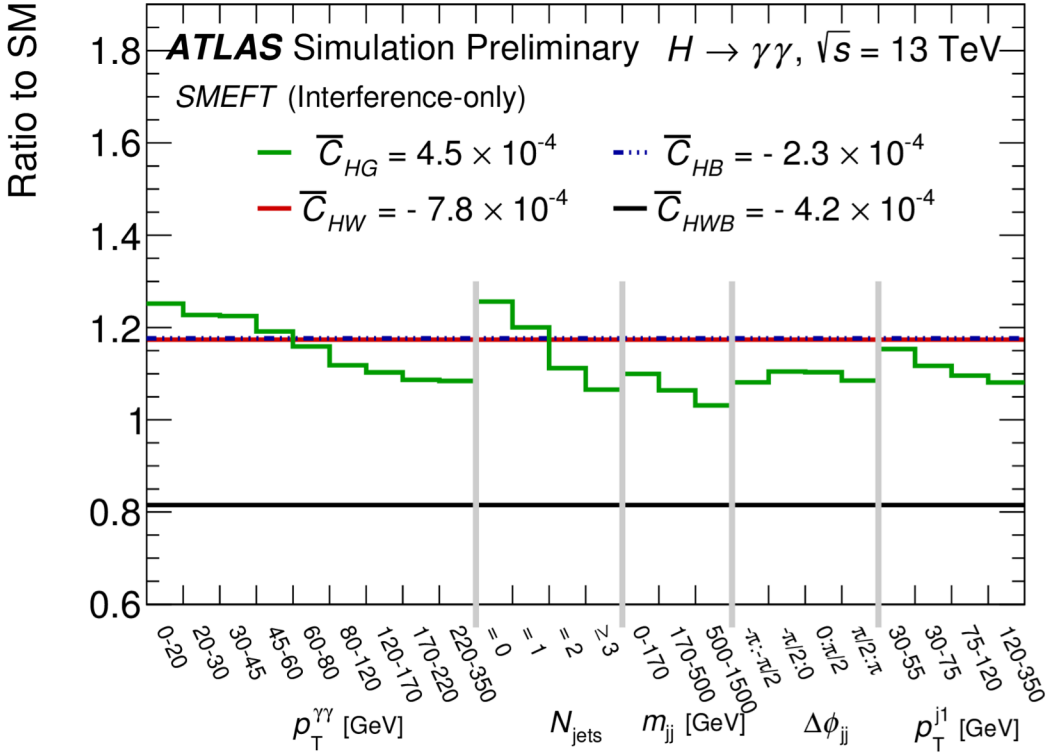

Charm Yukawa coupling

- Higgs to c-quark coupling is less constrained
  - VH(→cc) search, ATLAS (PRL120(2018)211802) : σ/σ_{SM} obs (exp): $110(150^{+80}_{-40})$
  - CMS (CMS-PAS-HIG-18-031): 70 (37^{+16}_{-10})
- Anomalous y_c couplings could modify Higgs p_T
  - Only the shape of the measured $p_T^{\gamma\gamma}$ spectrum is used, more model-independent

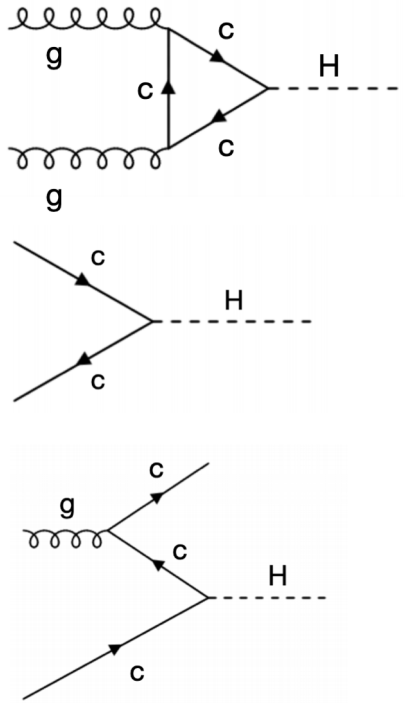

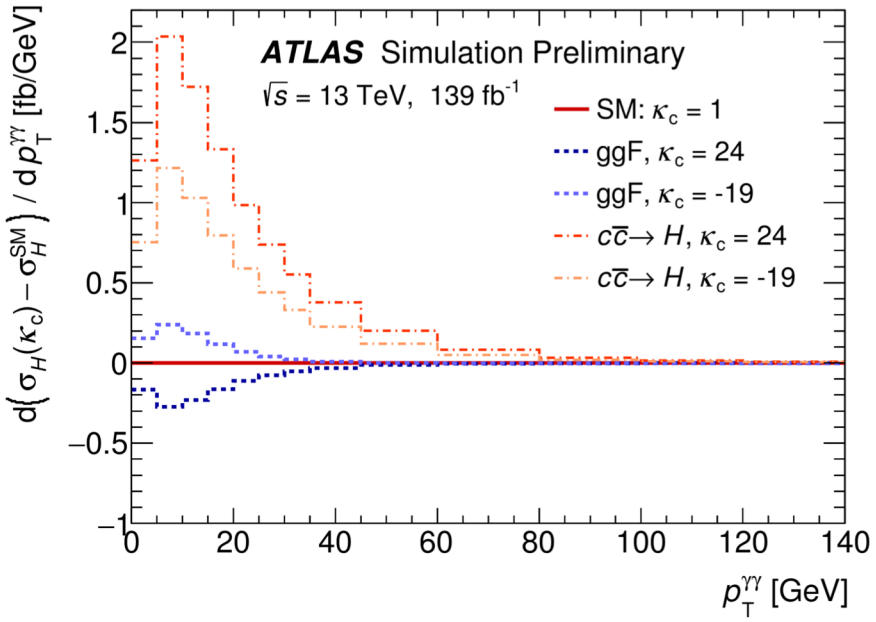

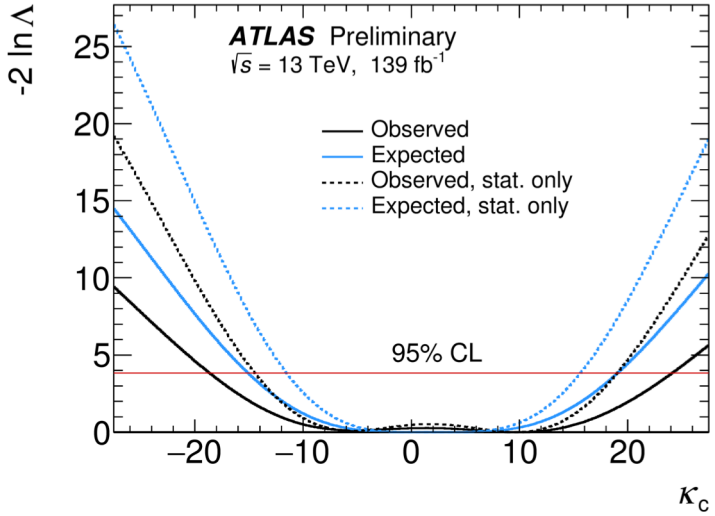

Coefficient	Observed 95% CL limit	Expected 95% CL limit
κ_c	$[-19, 24]$	$[-15, 19]$